Characterization of Granular Materials Using a Blade Hardness Gauge

by

Merieme Boutaib

Physical Sciences Department
Thompson Rivers University
Master of Science in Environmental Science

Supervisor:

Mark Paetkau, Teaching Professor, Physical Sciences

Committee members:

Thomas Pypker, Professor, Natural Resource Sciences

Jianzhong (James) Gu, Associate Teaching Professor, ARET

Thompson Rivers University

November 2022

Abstract:

This study was a preliminary investigation of the ability of a Blade Hardness Gauge (BHG) to reveal distinct behaviours in granular materials. A blade hardness gauge was constructed and used to investigate force versus time curves in dry/moist sand, polystyrene beads and snow. The effects of blade details, insertion speed (6-20mm/s), insertion direction (vertical or horizontal) of the blade were examined. There was a small but measurable effect on the blade details. The smaller cross-sectional area resulted in reduced forces. The insertion of blades vertically into dry sand is well described by an exponential force versus depth relationship, and importantly, independent on insertion speed. The vertical insertion into polystyrene beads shows a linear (weak exponential) dependence of the force as a function of the speed. The investigation into moisture laden sand shows an increasing force required for insertion up to about 20% moisture content, then decreasing back to dry sand equivalent for saturated sand (slurry). The use of the blade hardness gauge with snow revealed the force has a sigmoidal increase followed by a plateau, then an unexpected increase again. This preliminary study suggests the blade hardness gauge to be capable of identifying distinct granular materials and their behaviors, including moisture content and differences in snow layers

Acknowledgements

About 4 years ago I graduated from an engineering school in Morocco without really knowing what was going to happen next. The same year I had done an internship at University of Alberta which gave me a zest of doing research and coming back to Canada for another adventure. I decided to apply for a Master of Science in Environmental Science at Thompson Rivers University and start a new journey away from home. It turned out to be difficult and very different from what I expected. However, I am really happy that I have taken this step forward. This thesis is the result of the two years. Along the way many people have contributed directly or indirectly to the completion of this thesis. I would like to thank all of them.

First of all, my supervisor Dr. Mark Paetkau deserves the biggest recognition for giving me the opportunity to work under his supervision and introducing me to the research on granular materials. As a supervisor, he has been always patient, supportive and available, and gave me all the freedom I needed. As a person, he has been always kind, friendly and helpful. I learned a lot from him not only about science but also how to be a good person and make everyone love you. I would like also to thank the committee members for their interest in my research, and for providing me with their feedback also for their support.

Finally, I do not know how to express my gratitude to my parents Aziza and Larabi. Their unconditional love, sacrifice and prayers have been the biggest support throughout this journey. My Brother Adnane and my sisters Chaymae and Fatimaezzahrae, thank you for encouraging me and being there in my difficult times. This thesis is dedicated to all of you.

سبحانك يا ربنا لك الحمد والشكر حمدا كثيرا طيبا مباركا فيه.

الى المربيين الفاضلين الذين نسجا لي طريق النجاح في حياتي، اليكما ايها الوالدين الحبيبين، العربي بوطيب و عزيزة بوتمكرت.

الى اخوتي عدنان، شيماء وفاطمة الزهراء.

الى عائلتي بوتمكرت وبوطيب.

الى كل عزيز وغالي ساهم من قريب او بعيد في وصولي لما انا فيه.

احبكم جميعا.

Table of Contents

Chapter 1: Introduction

Granular materials play an important role in many industries and natural phenomena. Granular materials are found not only in pharmaceutical or mining but also in travelling desert dunes and earthquakes. Enhancing and handling the efficacy of the machines, or even constructing secured buildings necessitates a critical understanding of granular materials behavior. Conversely to what one might think about understanding granular materials behavior being a straightforward task, it has been only recently realized that granular materials cannot be easily classified as a solid, liquid, or even a gas, as they change states under slightly different conditions (Goncü, 2012). Granular materials have been the subject of in-depth engineering research for centuries. However, in the last two decades granular media has attracted notable attention from physicists, who have attempted to uncover the fundamental concepts needed to understand the complex behaviour.

Granular materials are understood as a collection of different macroscopic particles, for example sand, polystyrene, or peanuts in a container, or in geotechnical engineering as a composition of clay, sand, and gravel that appear in slopes, valleys, or riverbeds. Granular materials are especially used for the construction of earth-rock-filled dams, and other applications. It is known the granular materials behave distinctly from solids, liquids, and gases, this led some to identify granular materials as a new form of matter (Goncü, 2012). Although granular materials are relatively easy to characterize using density, particle size, etc., granular materials display complex behavior, the majority of which has not been satisfactorily explained (Carlson, 2008). Consider glass beads, a collection of glass beads have some characteristics of a glass block. Depending on the volume that glass beads might occupy, and the external force applied on them, the collection of beads behaves like solid, liquid or gas. For instance, when glass beads are constrained in a container, the compressibility is like a solid. On the other hand, when the container

is leaned the glass beads flow like a fluid. In the case of increasing the external forces (shaking the container), the glass beads will fly and bounce like gas molecules.

One of the studies that was relevant to this project investigated numerically and experimentally the influence of the particle size on the vertical plate penetration into dense cohesionless granular materials(Tanaka, 2019). In this study, they determined the impact of the particle size in the penetration resistance and the behavior of granular materials. Varying mean particle diameters (d50), but sustaining the same plate thickness, B, the research examined ratios B/d50 from 2.6-63. Particle size effects were exemained by conducting large-scale discrete element method simulations of vertical penetration into sand in quasi-two-dimensional conditions using 67.9 million particles (d50 = 0.233 mm). Their results mainly indicate the mean penetration resistance force surface rises when B/d50 decreases, whereas the tangential force applied on the side surfaces remain the same regardless of B/d50. Further the resistance increases linearly with penetration depth, while the tangential resistances increase with the depth squared.

Granular materials, like sand, have the ability to take the shape of its container, just as liquids do. It is essential to know the characteristics of granular materials, to avoid inefficient processing and avoid/predict catastrophic failures (avalanches). Equally important, granular materials behave distinctly when moisture is added. It is common to observe that beach sand, for instance, behaves differently than desert sand. This behavior is mainly due to the formation of bridges of liquid connecting particles and attaching grains together to form load-bearing structures. (Goodfellow, 2008)

Similarly, polystyrene as a granular material has been used in many fields such as insulation inside buildings. For this purpose, manufactures produce beads by supplying polystyrene with air, which leads to an expansion, resulting in a lightweight granular material. As
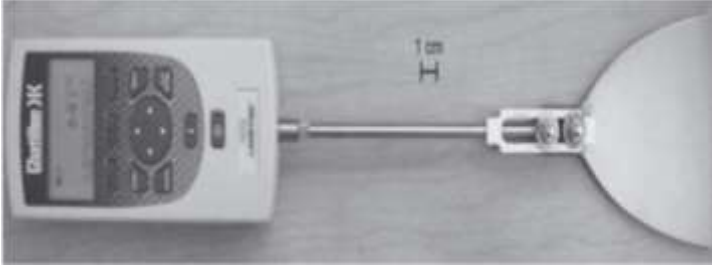
Figure 1 Blade hardness gauge, similar to the gauge used in this study. Modified from Borstad and McClung (2011).

well as other applications include containers, packaging, glazing, take-out containers and cassette cases. Polystyrene is also widely used as structural foam and expanded into beads for packaging and cushioning. For this project polystyrene was used as expanded beads, and especially for its lower density.

Snow cover and snow depth represent critical components of global and regional energy balances. An accurate characterization of snow behavior is important for hydro-electric operations, freshwater and land resource availability to communities, and prediction of climate change impacts (Way, 2021). The human ability to control in situ snow conditions has historically been restricted to open areas close to local communities. Hence, a detailed knowledge of the snow properties is important for diverse reasons such as avalanche hazard forecasting, or even the design of tire patterns for snowy roads. One of the characteristics of snow is its density; for newly fallen snow the density is approximately 20 kg/m^3 and for settled old snow the value is equal to 500 kg/m^3 (Stull, 2018). Since the snow has a low density, the shape and the bounding of an ice matrix can be changed easily. The low density of snow was a main reason for choosing polystyrene beads.

Granular materials, particularly snowpacks, have been studied using different experimental methods such as discs or shaft penetrometers or blade hardness gauges (BHG). These types of measurements date back to a push gauge tool invented in the 1940s using circular discs to measure

the snow hardness. The disc was accompanied with two types of gauges, one for the low hardness and the other for the high hardness. The size of the discs varied from 100, 10, 1 and 0.1 cm^2 and were pushed horizontally into the snow wall. The reading was obtained by slowly pressing the gauge against the snow and marking the value on the graduated scale at which the disc began to enter the snow. The hardness was obtained by multiplying the reading by the multiplying factor (Klein, 1950). Penetrometers have also been used to measure the snow hardness by vertical measurements into the snow wall. Whereas, as the penetration into the snow happens, a fracture in the snow will be generated. In order to improve on the design a thin-blade was created to examine penetration resistance in snow (Mcclung, 2011) Figure 1.

Measuring the resisting force of snow hardness is different from other classical granular materials. This is due to the combination of bond and grain ruptures, also the frictional rearrangement and compaction of loose grains around the penetrating object and friction between the snow and the penetrating object (Floyer J. &., 2006). Describing or knowing the contribution of each of the components of penetration resistance is far from understood.

Snow hardness is one of many measurements used to inform avalanche forecasting. Penetrometers can be used to measure the snow hardness. The measurements are carried out by vertically inserting the probe of the penetrometer in the snowpack. However, as the tip descends into the snow, a certain shape compaction starts to be created below and sideways from the tip, generating a perturbation in the snow prior to measurements (Floyer J. A., 2008) thus producing undesired spikes in the hardness gauging. Previous studies demonstrated that rounded and conical tipped probe penetrometers generate much larger zones of compaction in comparison with the blade tip. (Floyer J. &., 2006). The rupture of bonds and grains represents the most important element of hardness measures. The scale of interest for avalanche fractures is generally

investigated in (Borstad, 2010) study. They have found that shear and tensile fractures do not become critical until they reach a size of roughly 10-100 times the grain size. The other method used to determine the snow hardness is the hand hardness test. The hand hardness test requires a field operator to insert with a fist, four fingers, single finger, pencil or knife point into snow layers using constant force of about 15N. While the hand hardness test is currently widely accepted practice, it is not difficult to see it may be susceptible to bias: force amongst users, failure for the operator to consistently apply a precise value of the penetration force, inconsistent +/- scale and changing size of operator hand or glove sizes. The hand hardness test is typically susceptible to subjectiveness and depends on the user and challenges the reliability of measuring thin, soft layers of deposited snow. (McClung F. P., 2016).

McClung et al. developed and have been advocating a hand-held BHG (McClung C. B., 2010). In this device, a blade with width around 100 snow grains (10cm) was used to measure the penetration force. The BHG is intended to replace the hand hardness gauge. It provides an objective number and moves the bias from subjective measure of force to measure of insertion speed. This BHG has been shown to lead to enhanced agreement between field operators, when compared to the hand hardness method (Barsevskis, 2022). The final design of the BHG commercially available is a thin blade (100mm wide and 0.6mm thick) and was designed to be compact, reproducible, reduce snow compaction ahead of the penetrating tip and to evaluate resistance for a wider range of snow grains (10-100). The thin blade is also used to measure hardness in very thin layers of snow (weak layers). Results from previous studies (C.P. Borstad, 2011), (Barsevskis, 2022) demonstrated the thin-blade's ability to generate consistent data over numerous users with different penetration rates.

Scope and outline

This thesis offers a preliminary investigation of the behavior of different granular materials (dry sand, wet sand, polystyrene, and snow) using a BHG. In particular, we aim to investigate:

1. The effects of different blades: Is the measurement sensitive to blade details?

2. Effect of speed: Are BHG measurements dependent on insertion speed?

3. Is the BHG sensitive to different granular materials?

Through investigation of these questions, we would like to inform the use of the BHG in the field with regards to snow hardness measurements. Accordingly, the thesis is split in three parts (excluding the introduction and the conclusion chapters). Chapter Two contains an overview of the methods used and details of the BHG and preliminary measurements on the of dry/moist sand and polystyrene beads. Chapter Three then moves on to apply the measurement to snow samples. Chapter Four examines the effects of using the BHG as one would in the field, notably inserting the blade horizontally into polystyrene and sand. Finally, Chapter Five is a summary of the results and the analysis of the behavior of different granular material that we have seen in this thesis, and is accompanied with conclusions and further recommendations.

Chapter 2: Characteristics of the penetration force in dry sand, wet sand, and polystyrene

Far from being simple materials with simple properties, granular materials present an astounding range of complex behavior that defies their categorization as one kind of liquid or fluid. Just by considering how sand can stream through the orifice of an hourglass yet support one's weight on the beach. Despite considerable efforts, there still is no comprehensive understanding of these materials, as it is inherently difficult to characterize the particles of the granular materials solely and observe the dynamics of mesoscopic structures and individual particles in experiments. (Umbanhowar, 2000)

To better understand the behavior of the granular materials, the basic physical properties must be characterized. The properties examined in this work are particle size, density, and moisture content. Once a basic methodology of these properties is established, the chapter then discussed the details of the blade hardness gauge measurements and the application simple phenomenological models to analyze the BHG data. This chapter outlines methods used to investigate the BHG.

2.1 Methods

2.1.1 Materials

As this is a preliminary study, we used conveniently available materials to study: common playground sand and polystyrene beads. These materials were chosen for a number of reasons. First, the two materials have quite different densities (see below), and as this work is ultimately interested in the BHG as it relates to snow, a range of densities is useful. The second reason is particle size. Sand has irregular shaped small particles (0.05 to 1.2mm), while polystyrene beads have a range of sizes (1.2 to 3mm), but are primarily spherical. Snow also displays a wide range of particle sizes. Sand was sand-box sand available from The Home Depot, and polystyrene beads

were from a local department store (Lounge & Co. Beanbag filling). Later in this chapter we will examine the effects of moisture on the sand as well.

2.1.2 Particle Size

The particle size analysis of the sand and polystyrene has been carried out. The particle size distribution was determined by taking a small sample of the granular material and spreading it out on a surface to minimize touching/overlap. A photograph was taken (Figure 2A) of the spread-out material and then imported into image analysis software, ImageJ. A built-in function in ImageJ was used to identify the particles (Figure 2B) and then estimate the particle sizes. The output of ImageJ was then used to create a distribution, as shown in Figure 2 C. This was completed for sand (Figure 2) as well as polystyrene beads (Figure 3).

The average particle sizes for the sand ranged from 0.047 to 1.09 mm, with a mean of 0.310 ±0.012 mm, N=603, reported uncertainty is the 95% confidence interval. The peak in Figure 2 C at low radii (0.05-0.10mm) is likely due to the limitation of the pixel size of the raw image, so the distribution is likely artificially skewed away from gaussian. Similarly, the polystyrene particle size was analyzed. The raw photograph is shown in Figure 3A (black background was used). Figure 3B is the negative of the raw image and was used by ImageJ to determine the particle sizes. Figure 3C shows the particle size distribution of the polystyrene. The figure exhibits distribution as a bell-shaped (normal) histogram, ranging from 1.2 to 3.1mm giving an average polystyrene bead size 2.16 ± 0.11mm, (N=178), and the reported uncertainty is the 95% confidence interval.
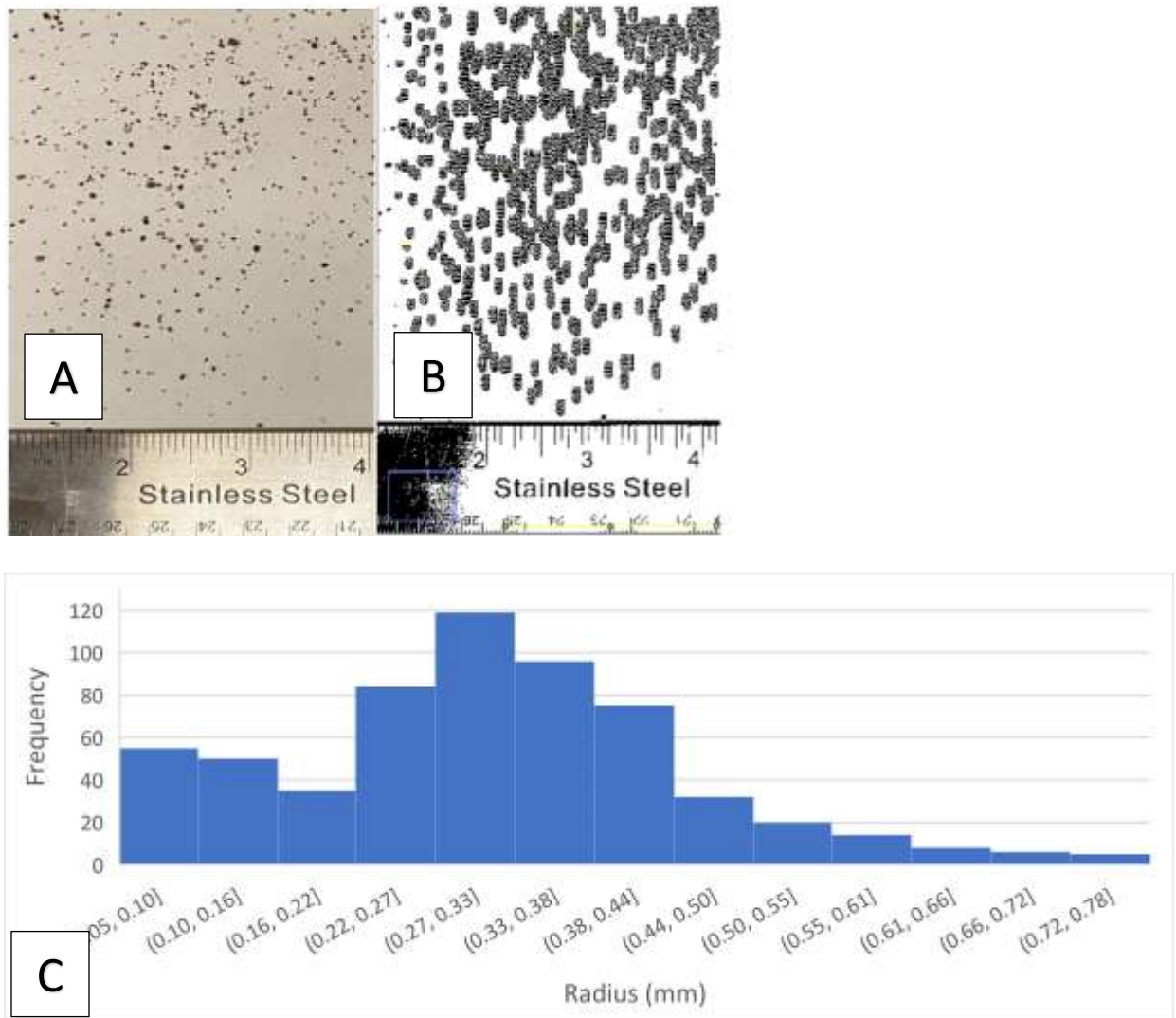
Figure 2 A. Raw image of sand particles Image of the analyzed sand particles accompanied with regular ruler for measurements reference taken using the camera. B. Image of sand particles assumed circular obtained using ImageJ. C. The distribution of the sand particles size skewed to the left due to the limited pixel size, with a peak at .4mm radius
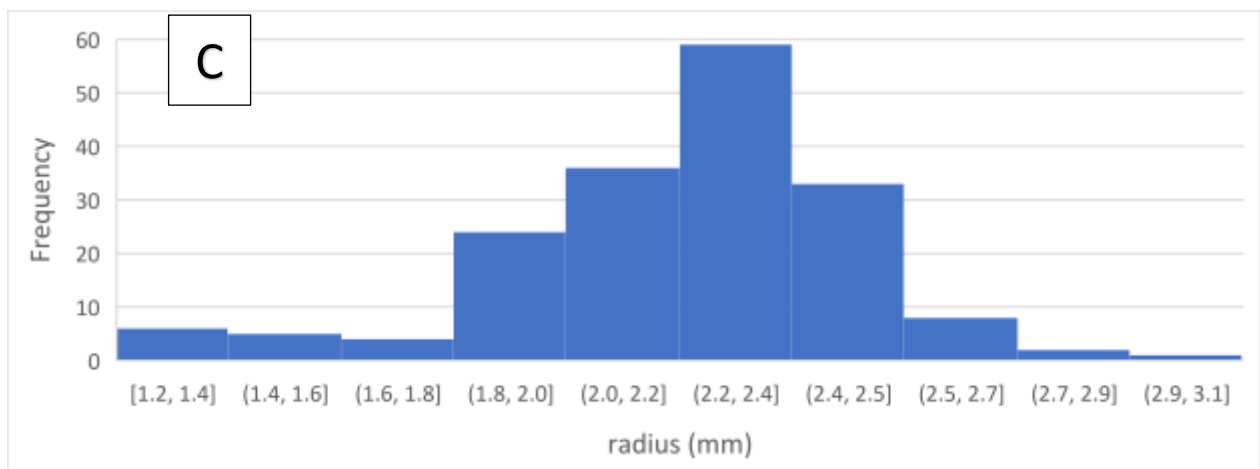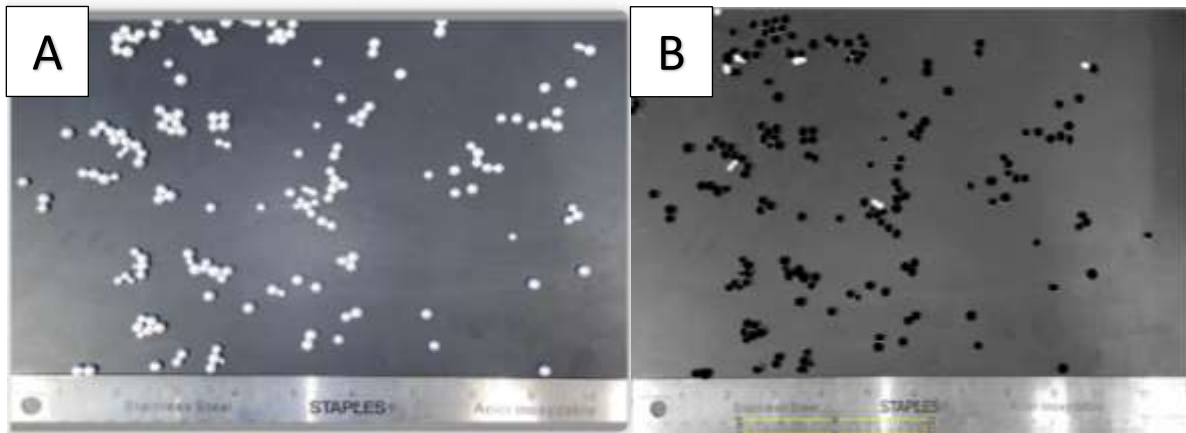
*Figure 3 **A**. Raw image of the polystyrene beads taken using phone camera. The ruler was used as reference for the measurements. **B**. Image of the polystyrene particles assumed circular obtained ImageJ. **C**. Distribution of the polystyrene particles size centered with a peak at 2.3 mm radius.*

2.1.3 Density

The density can be calculated using:

$$\rho = \frac{m}{V} \qquad (1)$$

where ρ is the density (in g/cc), m is the mass of the material (in g) and V is the volume of the material (in cc). In this work, we will define *density* as the density of the granular material, as opposed to the *bulk density*, being the density of the material making up the individual grains. As we are working with granular material, about 25% of the volume is unoccupied.

2.1.3.1 Methods & results

The density of the materials was determined in the following manner. The mass of an empty container was measured using a digital balance (ACCULAB VI-1200). Then 200 cm^3 of sand was measured into a standard chemistry beaker, and poured into the empty container.

The density was then calculated using equation 1. This procedure was repeated eight times (N=8) giving the average sand density of 1.59±0.06 g/cc.

As mentioned, polystyrene beads from (Lounge & Co. Beanbag filling) were used in this study. The bulk density of polystyrene is equal to 0.05g/cc (M.Haynes, 2020). The density of our beads was not directly measured.

2.1.4 Moisture Content

Sand and other granular materials are known to adsorb moisture from the air (Thom, 1970). This led us to investigate the approximate water content of the sand when it is exposed to the air in the laboratory.

2.1.4.1 Methods & results

We opted to determine the moisture content by weight loss upon drying. We started with a sand sample from the lab. These samples were weighted on a digital scale, then placed in an oven

at 360° C for 36 hours. The weight loss due to evaporation of moisture is recorded and the moisture content (MC) of the sample determined from:

$$MC = \frac{M_{ms} - M_{ds}}{M_{ds}} \times 100\% \qquad (2)$$

where M_{ms} is the mass of the moist sand and M_{ds} is the mass of the dry sand.

200cc of moist sand was poured into a beaker and baked in an oven at 200C. The moist sand mass was 317.9 ± 1.2g, (N=8), and the reported uncertainty is the 95% confidence interval. After spending 36 hours in the oven, the volume decreased slightly, and the mass of the dry sand was equal to 296.9 ± 0.1g. Applying equation 2 the moisture content which is found to be about 8%. From this procedure we also arrived at a density for dry sand of 1.48 ± 0.10 g/cc.
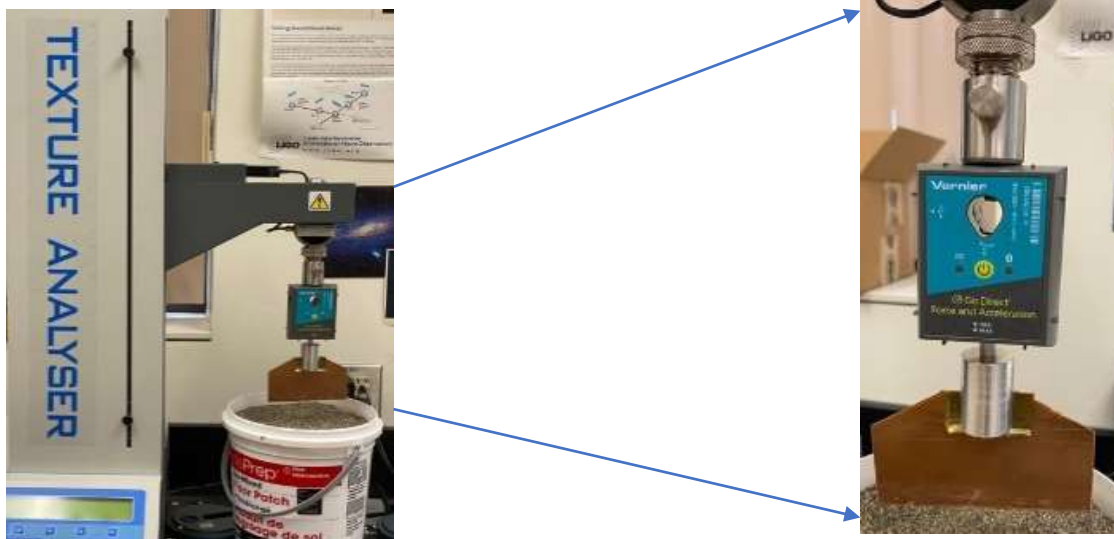

Figure 4. a) The Texture Analyser used to provide constant vertical speed. b) The force meter used to measure the vertical force on the blade.

2.2 Blade Hardness Measurements

Dry Sand

2.2.1 Materials

The TA1 texture analyzer device (see Fig. 4) is a device used for testing compression, shear, extrusion, puncture, hardness forces, etc. For our particular application, we used the TA1 to insert a blade into our granular material at a constant speed. The speed of the TA1 can be adjusted from 5.8 to 21.2 mm/s. To measure the force, a Vernier wireless Force meter was used. This force meter was attached to the texture analyzer, and a blade probe was attached to the force meter. A laptop connected via Bluetooth to the force meter and data was collected and analyzed using Vernier graphical analysis software. The above setup recorded the vertical force in the granular bed as a function of time. The sampling rate is 50 samples per second.

Four different blades were used to examine the sensitivity of the blades towards the granular materials. The blades were from three different materials but were all rectangular in shape. The details of the blades are shown in Table 1.

Table 1. Blade Details.

Blade	Length (cm) ±0.10	Width (cm) ±0.10	Thickness (mm) ±0.10	Cross section (mm^2)±5.0
Short copper	12	8.6	1.22	104.9
Long copper	15	8.6	1.22	104.9
Steel	10.4	4.9	0.32	15.7
Aluminum	11.5	7.9	1.04	82.2

2.2.2 Methods

Before each test, the blade was positioned at the top of the free surface of the granular material. For each type of blade, a different depth was set according to the blade length. so, the blade penetrates the granular material completely. e, g., in the case of the aluminum blade inside the polystyrene, the depth was equal to 130mm. For the long copper blade, the depth was equal to 100mm. Similarly, the stainless-steel blade in the dry sand had a depth equal to 95mm.

In order to test the values of the penetration force in the dry sand (figure 4 a), numerous trials were carried out using the force meter with an attached blade. Figure 4.b shows the short copper blade attached to the force meter at the free surface of the dry sand before insertion. By means of the texture analyzer, the distance between the blade and the free surface of the dry sand can be adjusted. After setting up the depth and the speed, the blade starts descending and making its way into sand. During the penetration of the blade, the Vernier graphical analysis software plotted the values of penetration force as function of the time. After a complete insertion of the blade into the dry sand, the blade goes back to the initial position.

2.2.3 Results

Figure 5 shows the force versus time data for the short copper blade at a speed of 8.3 mm/s. Blade penetration starts at about 1.8s and the increases with time (thin line). At about 5.6s, the collection run ends as the TA1 reverses its motion and extracts the blade from the material.

The penetration force has an exponential trend and has been fitted to the relevant data (thick smooth line). When the blade rises from the bottom to the free surface, disturbances of the vertical force profile are induced by its motion, and this led to more fluctuations. Between trials, the dry sand was mixed, and the bucket was shaken to maintain similar initial conditions. For each trial, an exponential fit was added as the best fit of the data. As shown in figure 5 the values of a, b, and c can be collected using the Vernier graphical software.

The measurements were repeated at the same speed, in order to test the reproducibility. Figure 6 shows six trials for the short copper blade inserted into dry sand at a speed of 11.7 mm/s. The data shows a consistent exponential behavior, but of course has variation.

The penetration force that was measured in the dry sand is equal to:

$$F(t) = F_0 e^{ct} + \beta \tag{3a}$$

Where F(t) is the force at time t, F_0 and β are fitting parameter (in Newtons), and t is in s and c is also a fitting parameter (s^{-1}).

A series of trials allow us to determine the average c, or $\bar{c}$ Now suppose we insert the blade at different rates or speeds, v. If we find $\bar{c}$ is proportional to speed, $\bar{c} = Bv$, by substitution into 2.1 then we find
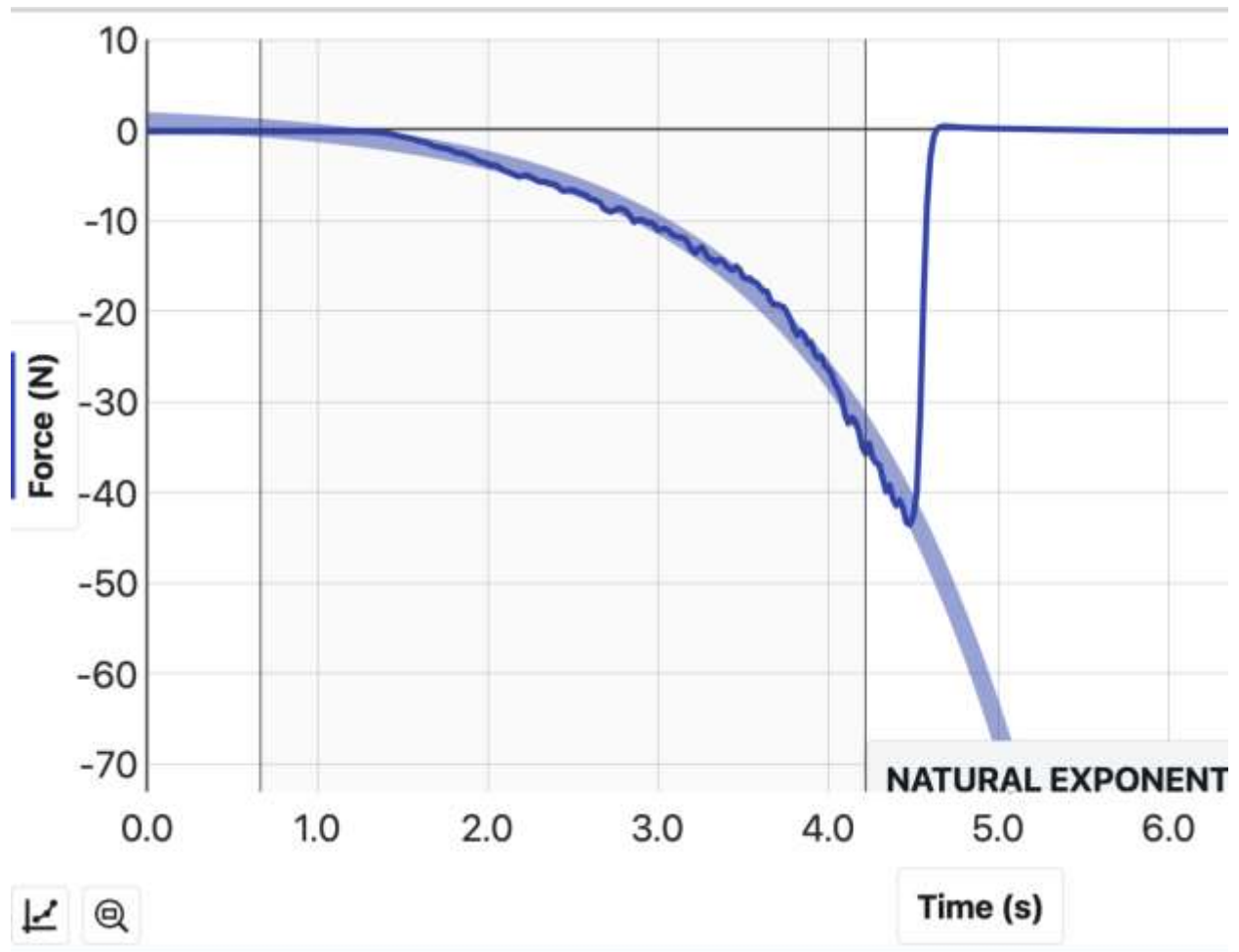
$$F = F_0 e^{Bvt} + \beta \qquad (3b)$$

Figure 5. Data from the lab evaluations in dry sand measured using Vernier force meter. The type of blade was the short copper blade, 12±0.10cm length, and 1.22±0.07 mm in thickness. The graph represents force versus time for a speed equal to 12.5mm/s. The solid blue line indicates the fluctuations of the force in the granular material, and the light blue line is an exponential fit to the

data curve. The blade starts penetrating the dry sand at approximately 1.8s, and it goes back to the initial position at 4.5s.
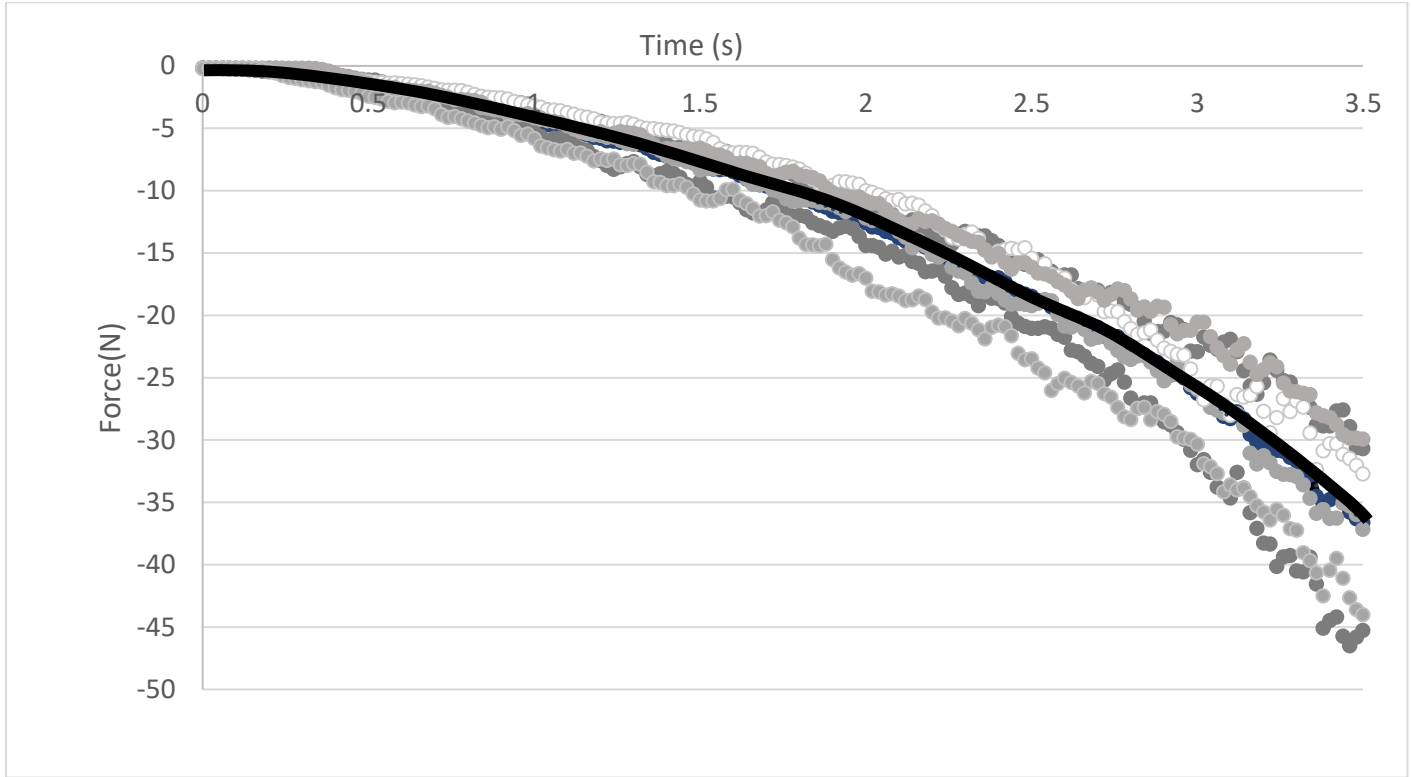

Figure 6. For six different runs, this figure exhibits the measured force as the blade is inserted at 11.7 mm/s. The solid line is the average of all runs; the average of c value is 0.56±0.08 s⁻¹. All trials display similar exponential behavior.

Which reduces to:

$$F = F_0 e^{Bx} + \beta \qquad\qquad (3c)$$

From the previous results of the dry sand, we can conclude that the penetration force increases exponentially with the depth until a maximum. To examine the effect of blade details, blades with different dimensions were used to measure the penetration force into dry sand and polystyrene. By calculating the average of c and plotting it as function of the speed (mm/s) we were able to get the results in Figure 7. The results in Figure 7 were assessed by using the aluminum blade into dry sand. Figure 7 shows average of c from equation (3a) plotted as function of speed (mm/s)
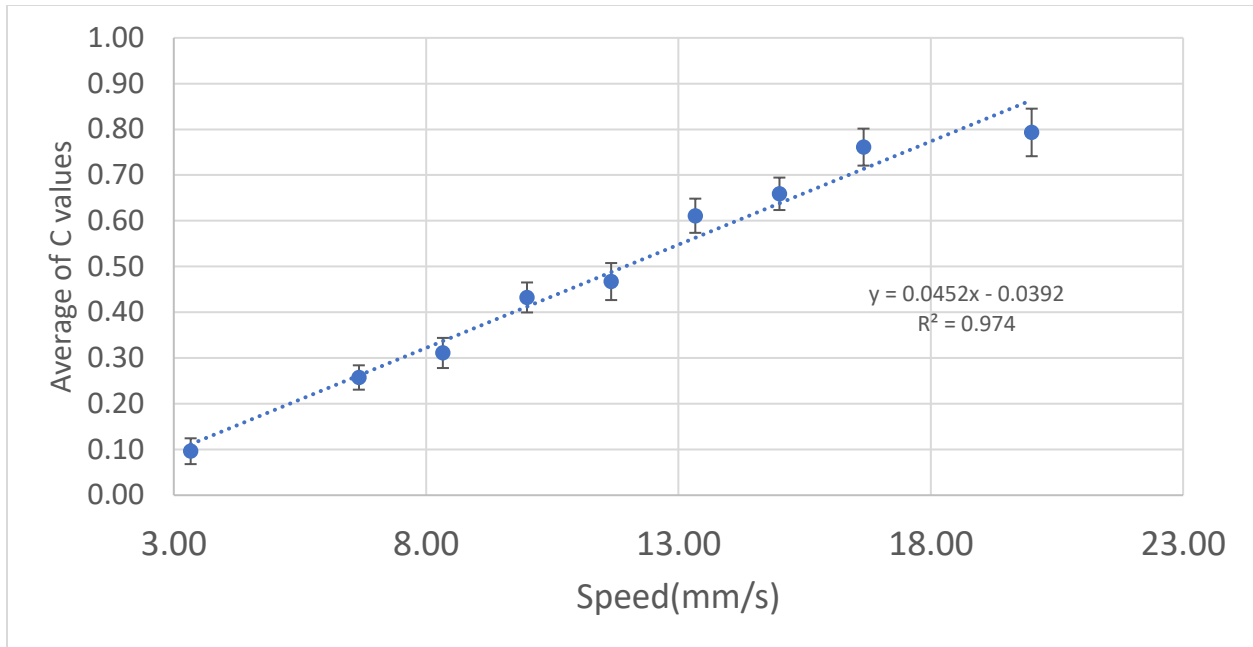
Figure 7. Average of c from $F=F_o \, e^{ct+\beta}$ plotted against the speed(mm/s) from the dry sand measurements using the aluminum blade (11.50±0.10cm length, and 1.04±0.01mm thickness). The dotted line is a linear fit to the data.
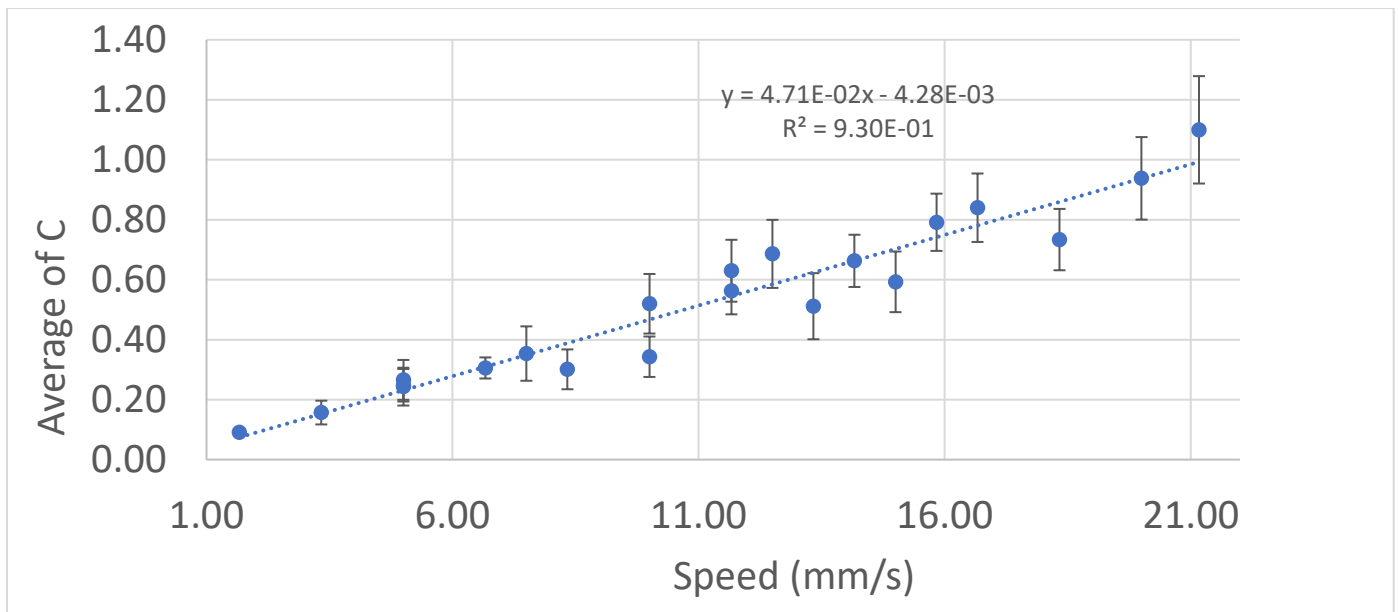

Figure 8. Values of $\bar{c}$ plotted as a function of the speed(mm/s). The measurements were performed by means of the short copper blade in the dry sand. The dashed line in the inset is the linear fit of this data.

into dry sand. In all of the speeds, the graph is following the linear fit. As could be expected, we can see variation in the trials as shown by the error bars.

The second blade that was used into dry sand was the short copper blade. More trials were carried out for this blade compared to the aluminum blade. Figure 8 exhibits the linear fit of the data showing the slope and the intercept, and the error bars which were 95% confidence intervals. The error bars are longer in the short copper blade compared to the aluminum blade which means that we are having more variation in the values of the average of c even if we took more measurements. However, such variations are expected in the trials, also most of the data points follow the linear fit.
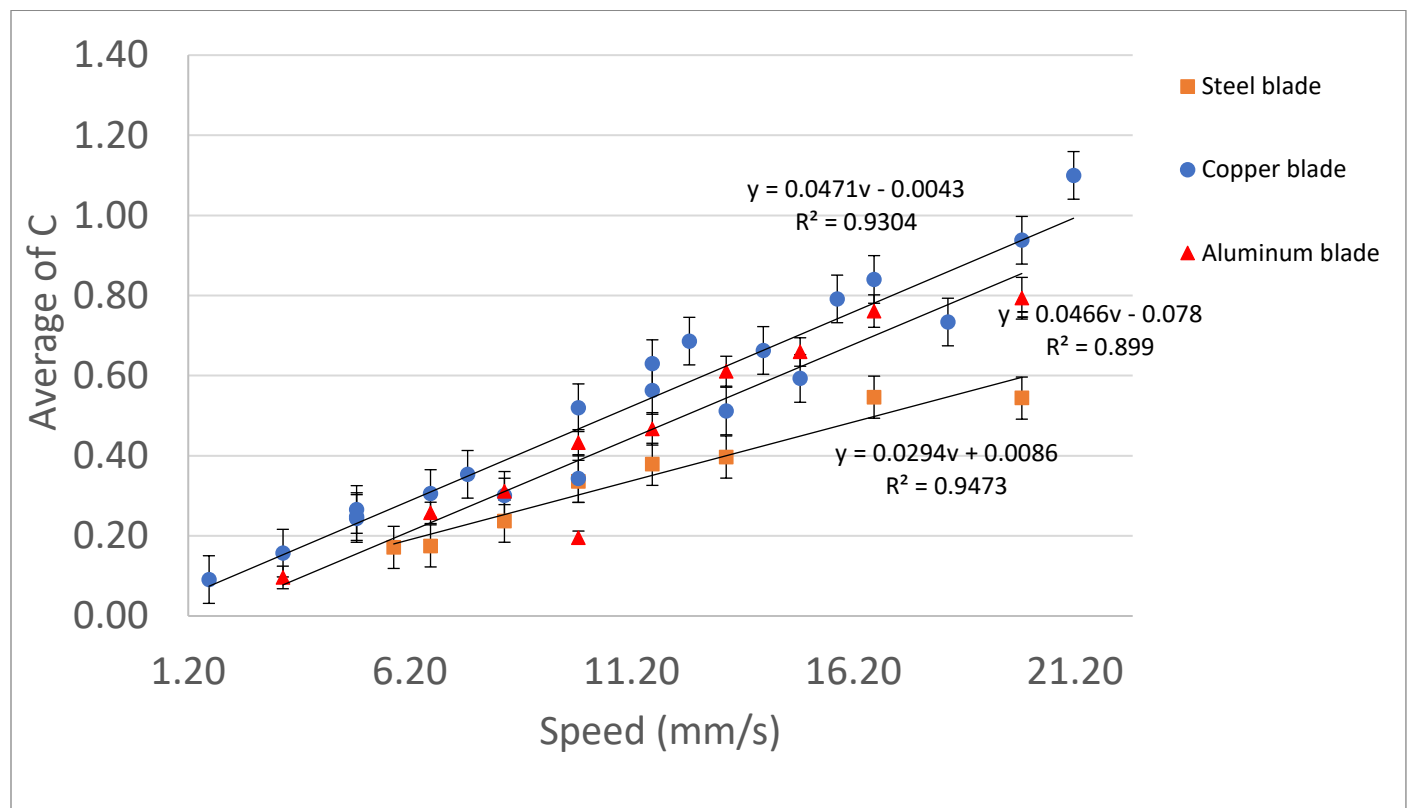

Figure 9. Averages of c from $F=Fe^{ct+\beta}$ plotted against the speed(mm/s) from the dry sand measurements using two types of blades (steel and copper), $\bar{c}$ had an increased linear trend in function of different speeds. The blue series represents data taken with copper blade; orange series represents data taken with steel blade. The data points fall significantly above the line as below the line. Both lines miss some of the error bars.

Figure 9 displays data taken using the steel, copper, and aluminum blades. Data are well defined by straight lines ($R^2 > 0.9$). The slope and the intercept values are similar between the aluminum and the copper blade with a lower value in the steel blade. For the aluminum blade graph the slope was equal to $0.046 \pm 0.0014\ s^{-1}$, and for the copper blade graph the slope was equal to $0.047 \pm 0.006\ s^{-1}$. The slope for the steel blade was equal to $0.0294 \pm 0.004\ s^{-1}$. In order to verify if the copper and the aluminum blades are similar or not, a simple t-test was applied using Excel. When comparing the aluminum and copper plates, the test results in p=0.39, so we cannot conclude there is a difference between the two measurements. This means there was no difference in slopes between the copper and the aluminum. When the t-test is applied to aluminum and the steel, p= 0.0031. We reject the null hypothesis of no-difference and conclude there is a difference between the slopes of aluminum and steel blades. Since c is reflective of the force required, copper and aluminum have a similar behaviour with respect to insertion force into dry sand (supported by the t-test results). The steel blade seems to require less force.

Polystyrene

2.3 Methods

The collection of polystyrene data was the similar to the dry sand. The main difference is the polystyrene was in a rectangular container, and, due to its low density, a top plate was added to allow compression of the system. In addition, two springs were used on both side of the container accompanied with brass shims placed under the springs to increase the compression. The length of both springs has an average of 18.65±0.70mm and experienced a compression force equal to 32.1±5.6 N, reported uncertainty is the 95% confidence interval.

The top of the box has two fine spaces to allow the blade to go through them and penetrate the polystyrene. Figure 10a shows a thin rod inside the polystyrene beads used to mix the polystyrene thoroughly. Figure 10b shows the two springs. Compression of the beads was controlled by placing brass shims beneath the springs.

2.3.1 Results

By means of the aluminum blade, we were able to collect raw data shown in figure 11. The graph follows a linear trend, especially if we focused on the graph between 5s and 20s. Towards the end of the graph and before the blade start coming back to the initial position, some fluctuations can be seen and that is likely due to the presence of larger grains at the bottom. For the purpose of testing the reproducibility of the measurements in polystyrene using the aluminum blade, several trials were completed for each insertion speed. Figure 12 shows ten trials for the long copper blade inserted into polystyrene sample at a speed of 5.8mm/s. The data shows a gradual increase in the force as the blade is inserted deeper into the sample box. The curve is not monotonically increasing, but shows structure, due to the particular random nature of the run, and likely due to these grains being much larger than the sand grains. Between trials, the

Figure 10. a) The polystyrene beads were placed inside of closed box. A thin rod was used to mix the polystyrene between trials. b) Springs were used on the lid to allow the beads to be compressed.
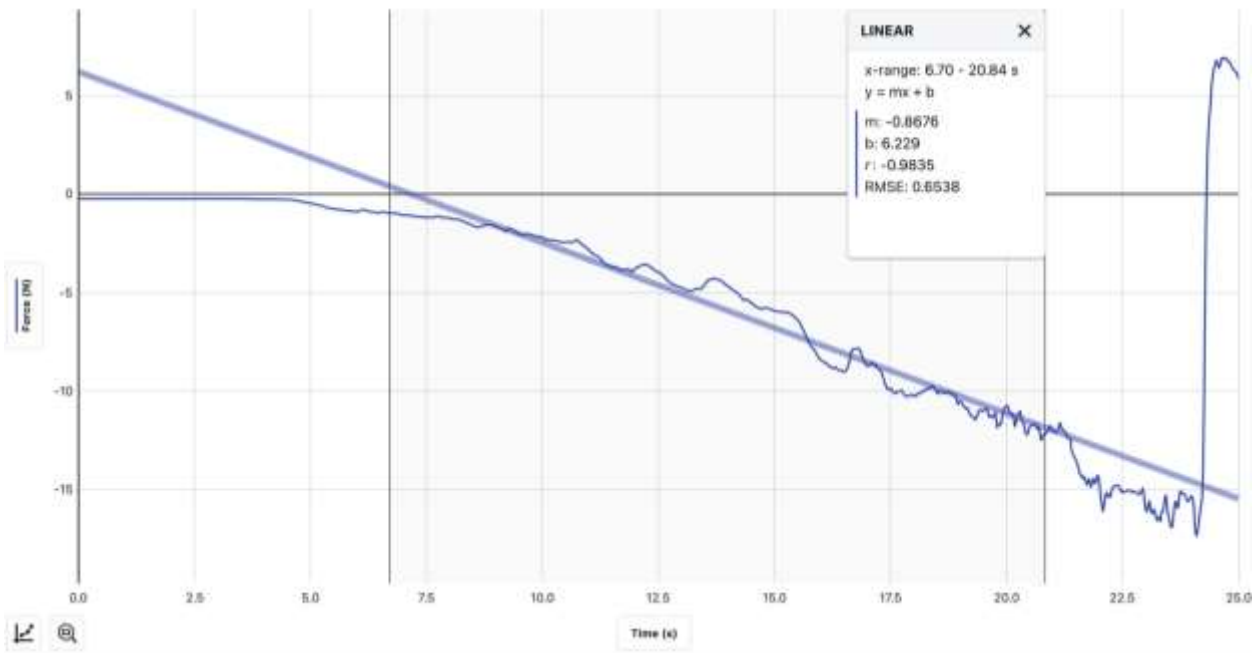

Figure 11. The resistive force (N) as a function of the time(s) at a speed of 3.33mm/s, a vertical penetration of an aluminum blade with a length equal to 11.5 $\pm$0.10cm, and a thickness of 1.04$\pm$0.01mm. The time between 0 to 5s, the graph is matching the 0 N force line as the blade was not inserted yet. After 5s the blade starts penetrating the granular material until time equal to 24s when it stops and goes back to the initial position.

polystyrene was mixed thoroughly. Not surprisingly, we see variation in the trials.   For each trial,

a linear fit was completed giving a slope and an intercept. This allows for the mean slope and

SEM2 to be calculated.
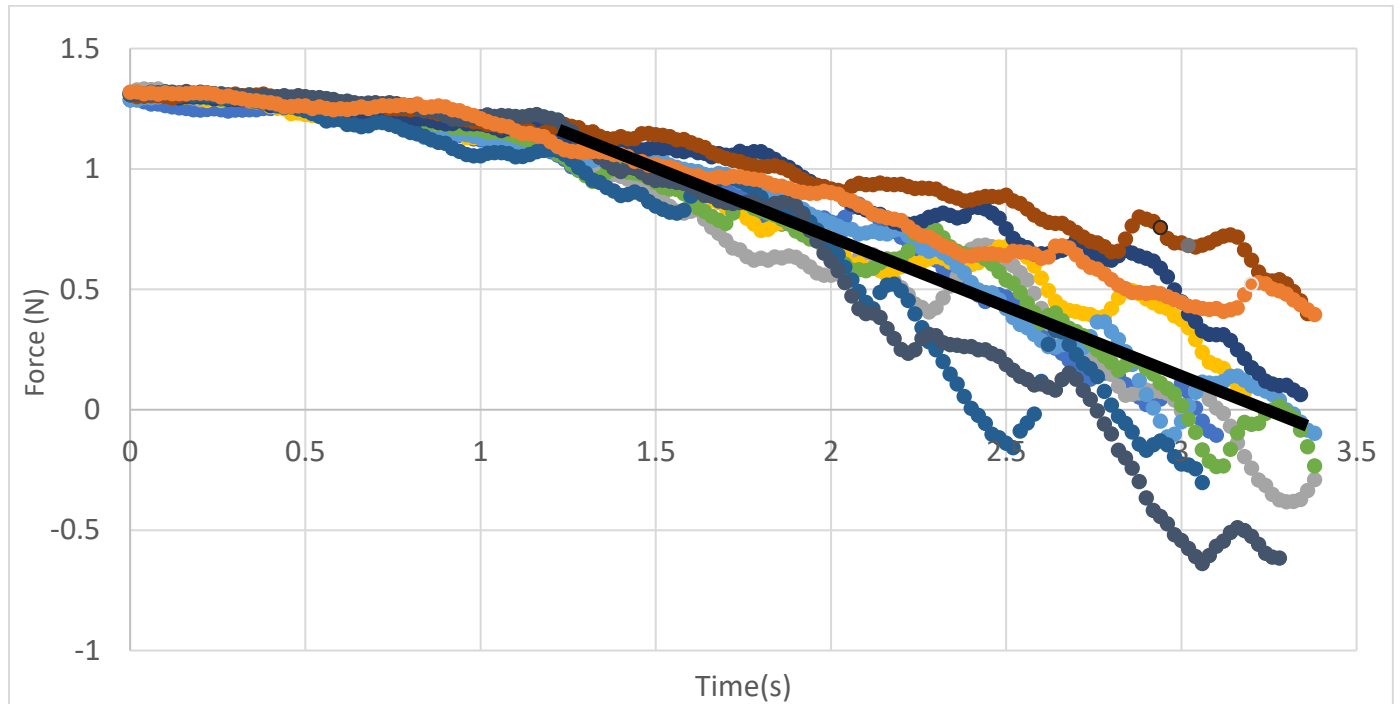
Figure 12. Using the long copper blade, in this figure there is the data collection of the force F in function of time in the polystyrene, at a speed equal to 5.83mm/s. For ten different runs, the trials show similar linear behavior with some fluctuations at the end. The thick line represents the linear fit of the average of the data.
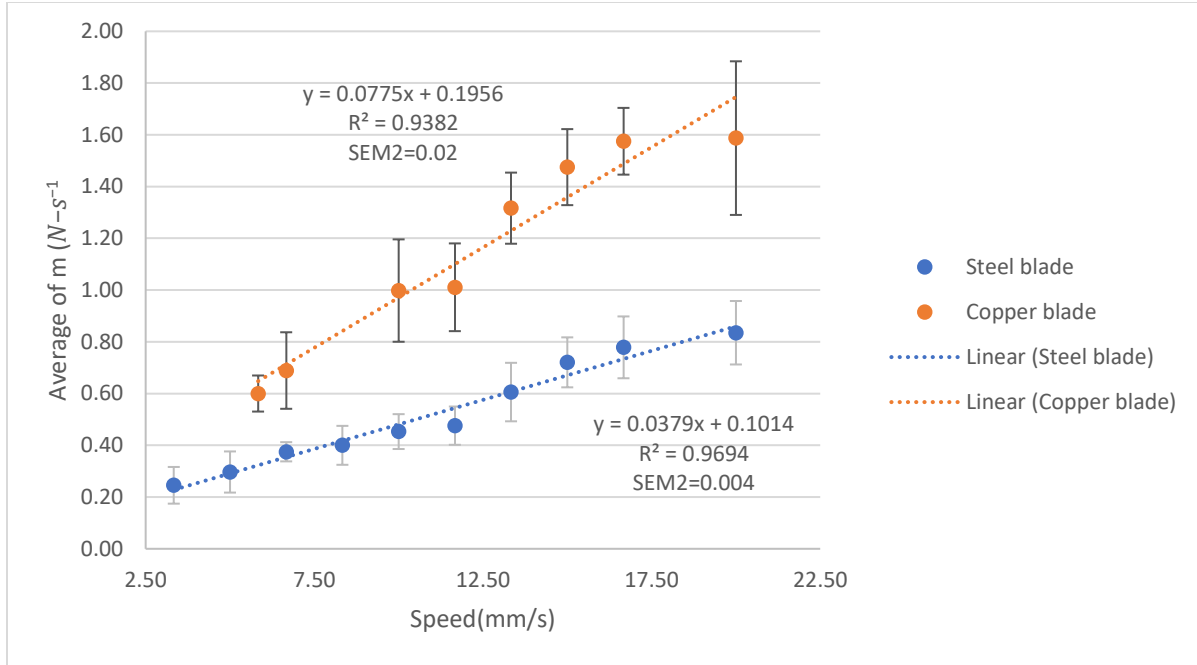
Figure 13. Measurements of $\overline{m}$ (Ns^{-1}) from $F = mt + b$ performed in the polystyrene, and by using the steel blade and the long copper blade. The dotted line is straight line fits to the data.

For low density materials, c might be very small, or the force might increase linearly in time.

$$F(t) = mt + b. \qquad\qquad (4)$$

where F is in N, m is in N-s^{-1} and b is in N. This leads to an investigation of the behavior of the penetration force into polystyrene.

The same procedure for the dry sand data collection was followed in the last figure using the long copper blade and steel blade. Multiple trials were completed for several speeds. Both data points follow the linear fit that was added in both graphs giving the slope: copper: 0.077 ± 0.020 Ns^{-1}and steel 0.0371 ± 0.0046 Ns^{-1}. A t-test confirms these slopes are statistically different, with p=0.066.

The graph of m versus insertion speed is linear, then we arrive at

$$F(x) = B'x + b. \qquad\qquad (5)$$

where F is in N, B' is in N-m^{-1} and b is in N.

Wet Sand

So far, the granular materials we have investigated can be described as cohesionless, i.e. there is no attractive force between individual grains. In this section, behavior is investigate as the water content of sand sample is changed. Can the BHG differentiate between a cohesive and non-cohesive granular material (dry and wet sand), and what happens as more water is added? As water is added to sand, the water will look to contact as much solid surface as possible and hence will gather preferentially at the points of mutual contact between adjacent grains (Herminghaus, 2012). A free water surface will consequently extend from one grain to the other, exerting an attractive force on the grains. By means of the BHG, the force in the wet sand was measured and the results were compared to the dry sand graphs.

2.4 Methods

The same method used in dry sand is used in this experiment as well, employing the short copper blade. Sand samples of moisture content 9%, 14%, and 19%, were created by the following process. The sand was first kept overnight in an oven preheated at 250°C to dry it before adding moisture. In order to moisture the sand equally, sand was split into layers. Half of the water was added to the 1/4 of the dry sand quantity, mixed very well using a spatula in a separate container, then mix the dry with the wet of sand. This operation was done twice to obtain a combination of a dry layer then wet layer, and again a dry layer then wet and later mix the material very well. The initial weight of the dry sand was 2400±1g, and 244.2g of water was added to the sand representing a 9% moisture content. Then 160g of water was further added to create a 14% moisture content sample. Finally, another 160g of water was added to get 19% moisture content. The 19% samples were essentially mud.

2.4.1 Results

As previously, multiple trials were completed for each insertion speed. Figure 14 exhibits the results of the blade insertion at a speed of 20mm/s into 19% sand. Figure 14 shows again an exponential increase in the force as the blade is penetrating. Between trials, the container was
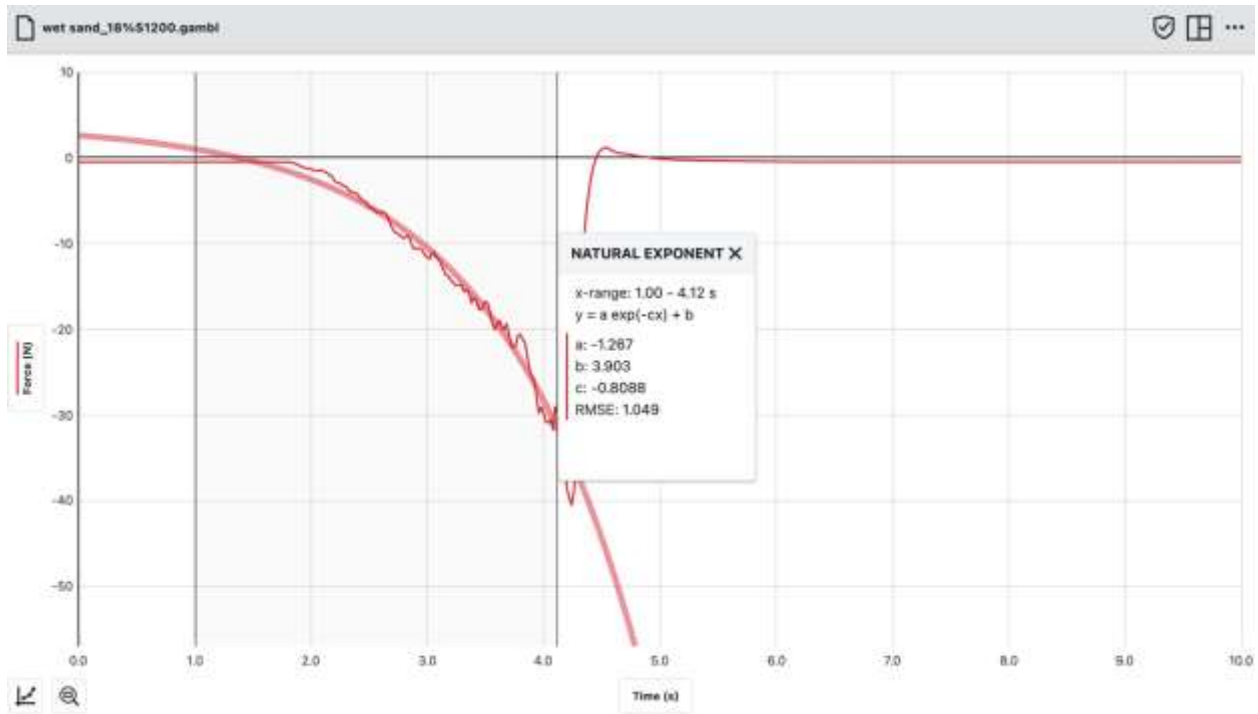

Figure 14. The raw data of the resistive force (N) as a function of the time(s) at a speed of 20mm/s in wet sand (content of the moisture is 19%). The time between 0 to 1.8s the blade was not inserted yet. Between 2s and 4.3s the blade was inside the wet sand.
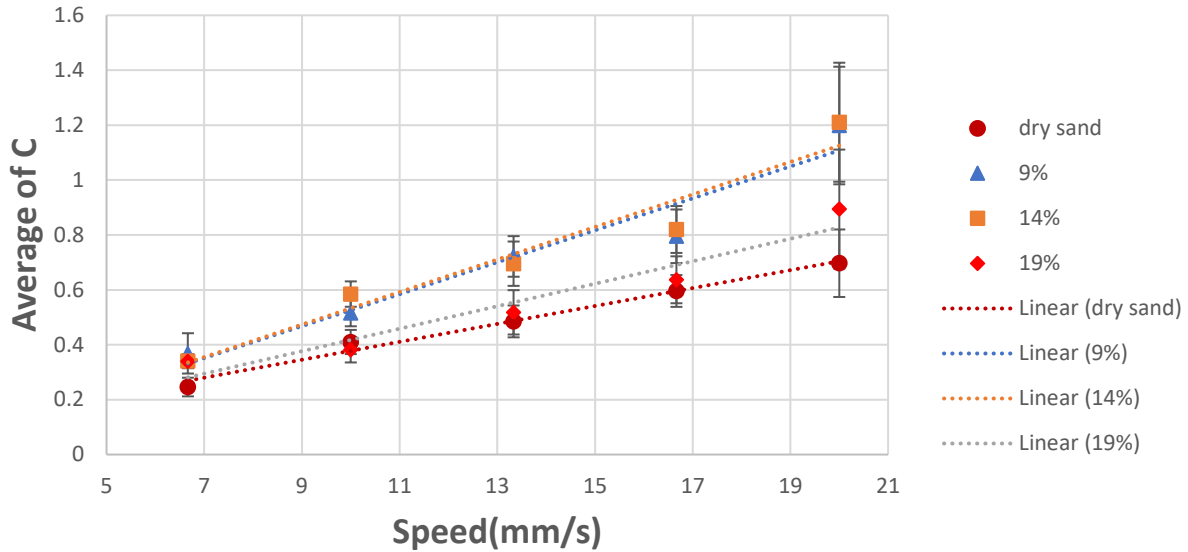
Figure 15. Results of wet sand measurements moisture at 9%, 14%, and 19%. Average of c (s⁻¹)
was calculated based on the c values in figure 12 and plotted as function as the speed (mm/s). the
linear fit of the data was added, as a guide for the eye, to follow where most of the same percentage
of data is located.

stirred to mix the sand. Measurements of the resistive force inside the wet sand containing 9%,

14%, and 19%, respectively, was recorded at speeds ranging from 6.66, to 20mm/s. Figure 15

shows the average of c values from the force versus time graphs plotted versus insertion speed.

The dotted lines represent the best fit of the data, and are again linear. A linear regression was

completed for each set of data. Dry sand data were added to the graph to compare between a totally

dry sand (0% moisture) and the other percentages. As it could be seen in the figure the force in the

dry sand has the lowest value, then increased at 9% (highest value at 13.33mm/s). A maximum

slope was registered at 14% moisture content, and when the wet sand starts becoming a mud at

19% the resistive force decreases and the values are close to the dry sand measurements.   A t-test

for the dry sand and the 14% sand samples gives a result of p=0.12. While this is not enough to

reject a difference, it does support a difference at the 88% level.

2.5 Summary

In this chapter we have described how to complete the basic measurements involved in this study, as well as made vertical blade insertion measurements on dry/moist sand and polystyrene bead. In addition, this chapter looked at the resistive force is characterized in two granular materials: sand and polystyrene beads. In the case of sand, the force versus time graph is well described by an exponential curve. In the case of polystyrene, the force versus time graph is linear (weak exponential). When the effect of insertion speed is examined, we find the parameters describing the forces depend linearly on the insertion speed, leading us to conclude the force essentially depends only on the distance into the material. The results of dry sand are in agreement with work done by (Tanaka, 2019).

The data show changing blades has a small effect on the BHG results. Considering only the cross-sectional area of the blade, the steel blade has 15% of the area of the copper (i.e. 85% less). This leads to about a 50% change in the slopes of Figures 9(sand) and 13(polystyrene). The Al blades have smaller area than copper (20% smaller), but no difference is detected. It is possible these differences may be due to other than cross-sectional area, such as material roughness, however this was not investigated. For more convenience we will be using the short copper blade for further measurements, especially that it has higher sensitivity, and its size is more suitable for force measurements. As the previous results prove that the force measurements are sensitive, we opt for examining if the blade can detect changes into different case of granular material (wet sand).

Similarly, the BHG proves to be able to characterize the behavior of wet sand and detect changes in force profile with small changes in cohesive forces. These preliminary results lead towards the capability of the BHG in investigating details of snow layers and snow behavior.

Chapter 3: Snow Measurements

Snow properties can be measured by using remote methods such as sensors mounted on satellites and airplanes, providing larger spatial coverage when compared to physical measurements. Yet, remote sensing is known to have great uncertainty in estimating snowpack properties at the relatively fine spatial and temporal scales by which they absolutely vary. (N. J. Kinar, 2015). Hence, a more precise method is needed to examine snow properties.

The widely known method of measuring the snow hardness is the hand hardness test (Quervain, 1950). Although it is easy use and execute, this test has limitations such as inconsistency between observers and lack of quantitative data. At the same time, the hand hardness test is frequently known to encounter difficulties in determining the hardness of thin layers, because the test requires the penetration of several objects into the snow, which are generally thicker than the weak layer itself. As a consequence, the hand hardness test provides only a rough estimation of the hardness difference between layers. To overcome the complications of the hand hardness test as well as other hardness tests, Borstad and (Mcclung, 2011) developed a thin blade.

3.1 Materials

In this chapter we will investigate the response of snow to the BHG measurements previously described. Snow was collected during three different months (January, February, March), and from different locations (around Kamloops). Ideally measurements would be made in the field, but moving the measuring equipment proved too cumbersome. Choosing snow from different locations and during the coldest months in Kamloops was with the intention of testing the capability of the BHG in detecting the hardness of several snow layers.

Is the BHG capable of characterizing the snow properties? Can the BHG differentiate between snow layers?

3.1.1 Density

Different from ice, snow has variable compressibility and high porosity. Due to the ability of snow particles to encounter change themselves, distinguishes and makes it a unique and distinct from other granular materials studied this far. Snow has a relatively low density owing to its

Figure 16 shows the square cylinder used to measure the density of the snow. Once the cylinder was filled, the mass was determined.

large pore spaces (McClung & Schaerer, 2006). The density, similar to other snow properties, vary through time under the impact of external factors, including temperature and the weight of the overlying snow layers (McClung & Schaerer, 2006). Previous studies have shown an empirical relationship between BHG and density measurements (Barsevskis, Oct 2022).

As seen in Figure 16, a hollow square cylinder (V = 70.00±0.020 x 23.50 ± 0.020 x 23.50±0.020 mm^3 = 38657 $\pm$ 46 mm^3) was used to estimate the density. The mass of the empty square cylinder was obtained using the compact digital balance (an ACCULAB VI-1200 laboratory small balance). With a known volume filled, equation 2.1 was used to calculate the density of snow sample. Typically, between 3 and 10 density samples were obtained; results are shown in Table 2.

Table 2. Density of Snow Samples

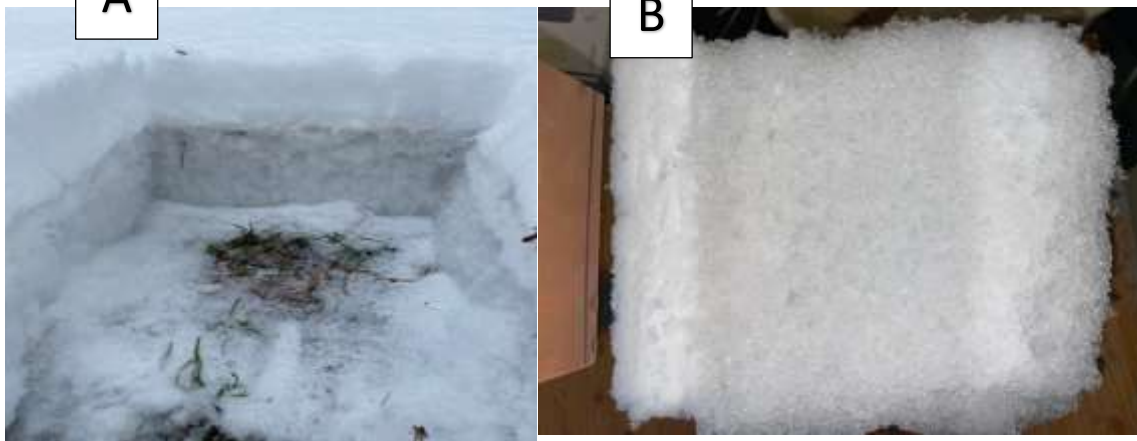| Layer	Density (± 0.02 g/cm^3)		Sun Peaks	Stake Lake
	Campus			
Top layer	0.32	0.41	0.59	0.47
In between	0.37	0.46	0.65	0.47
Bottom layer	0.46	0.49	0.62	0.50

Figure 17. Example of snow sampling. A) Shows the cross section of cut section. B) shows an example of snow sample used for the BHG measurements. This sample had dimensions (20 x18x16 cm³). The long dimension is perpendicular to the layers.

Snow profiles are commonly known to be the only means of obtaining a detailed picture of snowpack layering and bonding. To adequately capture the characteristics of an area of interest, it is common practice to collect snow profile information from different locations and employ targeted sampling to address specific hypotheses. When observing a snow profile, it is important to select a representative site first, because it plays a huge role in recording the layer characteristics. (Ju ̈rg Schweizer, 2001).

3.2 Methods

In order to obtain snow samples, a pit was excavated in the snow. Density and hand hardness are measured as a function of depth through the snowpack. Ideally this project would take blade hardness gauge measurements in the field, however a device to properly control the insertion speed was beyond the scope of this work. Instead, the snow was brought from the field into the laboratory.

Most of the experiments were done in snow that is well bonded with different layers that could be seen by eye, figure 17 exhibits different layers of snow collected for measurements in this study, as it shown in the picture the eye can differentiate two layers (hard and soft).

In the winter of 2022, fieldwork was executed in areas around Thompson Rivers University campus and around Kamloops. The choice of the snow locations was made based on the location slopes and elevation. The higher the elevation, the deeper the snow, and presumably this snow will contain older snow layers. The goal is to investigate several kinds of snow layers. At each location, snow samples were cut into approximately equal profiles (usually into square shape). Figure 17 shows one of the locations from where we collected our samples. Using a shovel to get a flat surface, and a saw to cut equal cubes of snow samples. The samples were approximately 16.8 cm in width and 21.8 cm in length. The full depth of the snow was used. Max depth of snow was 45 cm.

Cut as in figure 17 B, samples were placed into a big cart and transported close to the physical sciences research lab and tried to keep them in the outside temperature in order to sustain the initial state. Next step is moving them to the lab, then inserting the blade into snow, and collect data of the force at different speeds. (More details regarding the resistance force measurements can be found in chapter 2).

Starting with maintaining the same speed for the same snow layer in different samples. The aim was to examine the efficiency of blade hardness gauge differentiating between several snow layers. The hardness was measured in the top and the side wall of the snow samples (figure 17) the snow samples' measurements were an average depth of 10 cm (the measurements depend on the snow sample and weather conditions). To obtain the hardness, the blade was simply pushed 3-5 cm into the snow sample, parallel to the layering at a constant speed ranging between 4.17mm/s and 20mm/s. The graph of the resisting force can be read from the Vernier software downloaded in the laptop. For each graph, the mean value of the resisting force was collected into excel
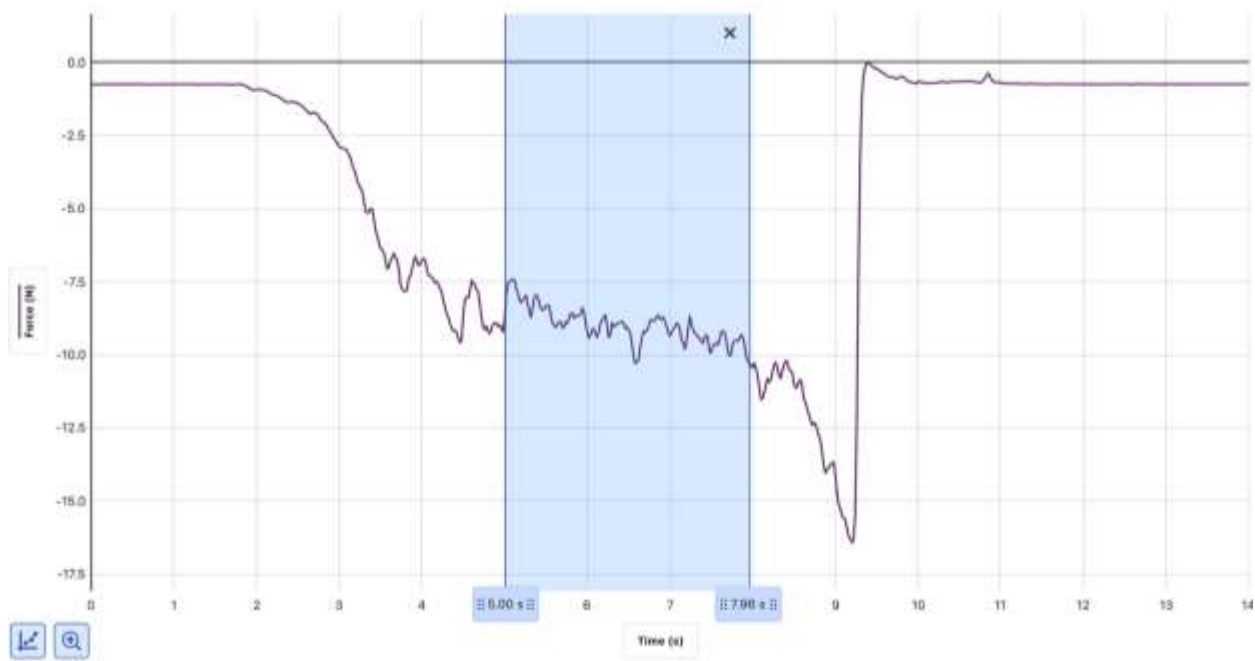

Figure 18 Example of raw data of the blade hardness gauge inserted at a speed of 6.7mm/s into a hard layer of the snow sample. The type of blade was the short copper blade, 20.00±0.10mm, length, 14.44±0.10mm, thickness. The purple line indicates the fluctuations of the force in the snow sample, and the blue highlighted area is where the plateau was detected. The blade starts penetrating the snow sample at approximately 2s, and it goes back to the initial position at 9.3s.

spreadsheet for later analysis.

3.3 Results

Figure 18 shows the force versus time data into the hard layer of a snow sample taken from campus area. Data were collected using the short copper blade at a speed of 6.7mm/s. Blade penetration starts at about 2s and increases with time. At about 5s, we can see the start of a
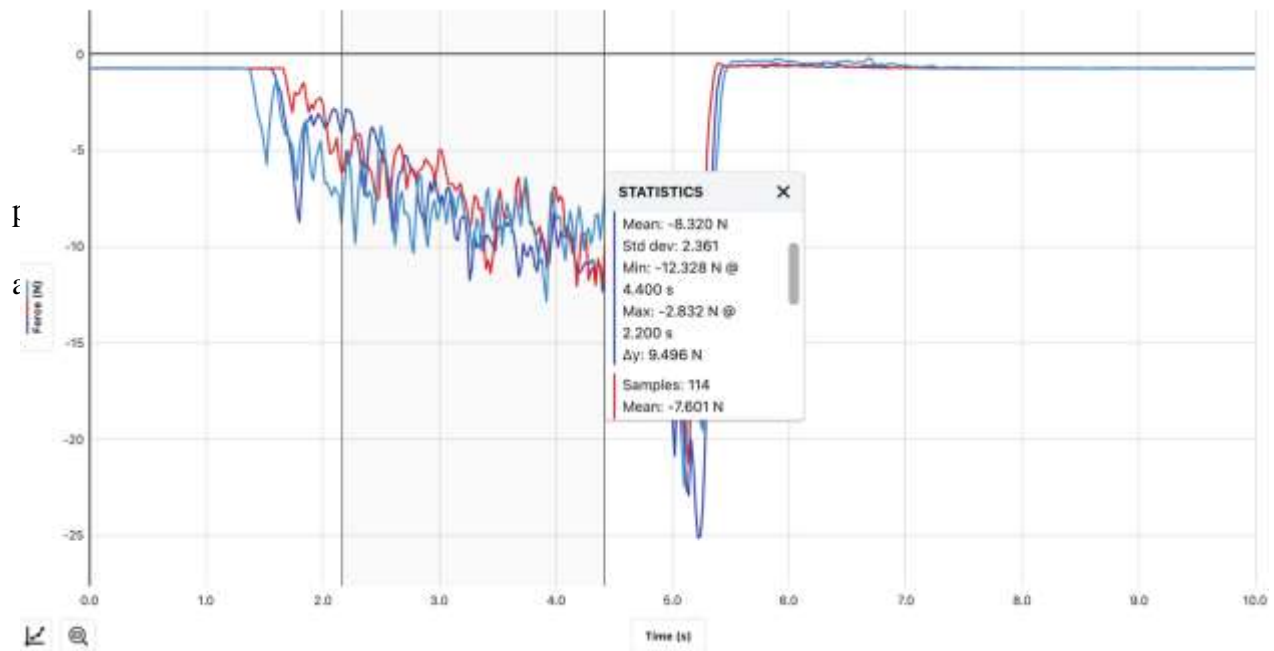
Figure 19 For three different trials, this figure exhibits the average of the plateau of the three trials displayed in three different colours using the Vernier software. the speed of penetration is 13.3mm/s into the hard layer of the snow sample collected from campus area.

We can clearly see an exponential increase leading to plateau, then after the plateau another increase of the force again. In all measurements, the blade did not miss any side of the snow layers and was thin enough to go through the hard layer. For each trial, the average force in the plateau region was determined.

Figure 19 is another example of snow collected on the TRU campus, showing typical reproducibility of the method. This data was taken with short copper blade inserted into the same snow sample at 13.3mm/s. The mean of each plateau for each trial was collected (three different colors and their correspondents means displayed using the Vernier software).

For all the three trials the blade was easily going through the sample and into distinct position (once the blade has been inserted in position 1 for example, it will not go through the same position again). While there is some variation in each trial, the plateau force is consistent within the different trials.
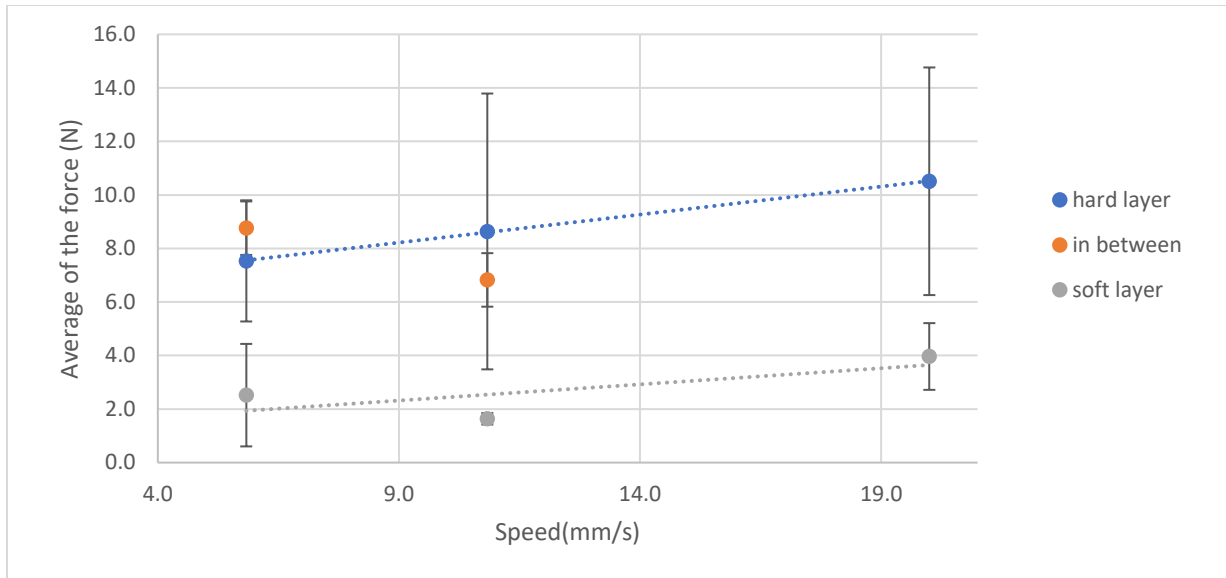
Figure 20. Average of the means of the plateau for each trial in three layers of the snow sample collected from the second site around the campus. The measurements were carried out at a speed between 5.8mm/s and 20 mm/s.

In order to investigate the capability of the BHG differentiating between snow layers, and its dependence of blade speed, the same procedure was repeated for a variety of blade speeds. These results are shown in Figure 20, which shows four different identified layers all using the short copper blade, and all collected around TRU. Snow samples were collected from around the campus with three visible layers named following the order they were noticeably distinct: soft or top layer followed by in between layer, and then the bottom or hard layer). Figure 20 shows the averaged plateau force for snow is almost independent of speed. We also see in this data larger variance, which is mostly a function of smaller sample size. The hard layer does reflect larger forces needed to insert the blade, compared with bottom soft layer but the difference is not large, and diminishes with increasing blade speed. The linear fits are passable representations of the data, certainly not as good as from sand and polystyrene results.
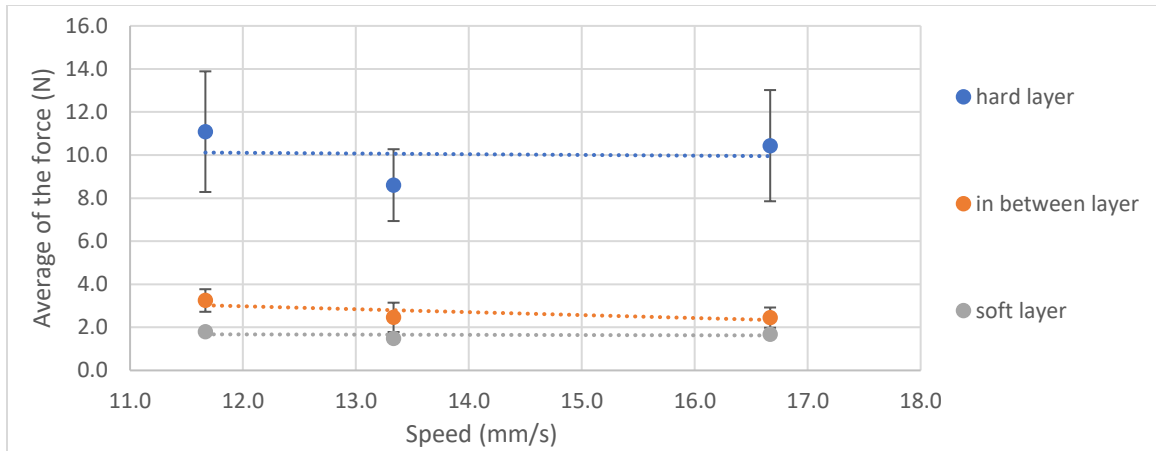
Figure 21. Average of the means of the plateau for each trial in three layers of the snow sample collected from the third site around the campus. The measurements were carried out at a speed between 11.7mm/s, 13.3mm/s, and 16.7mm/s.
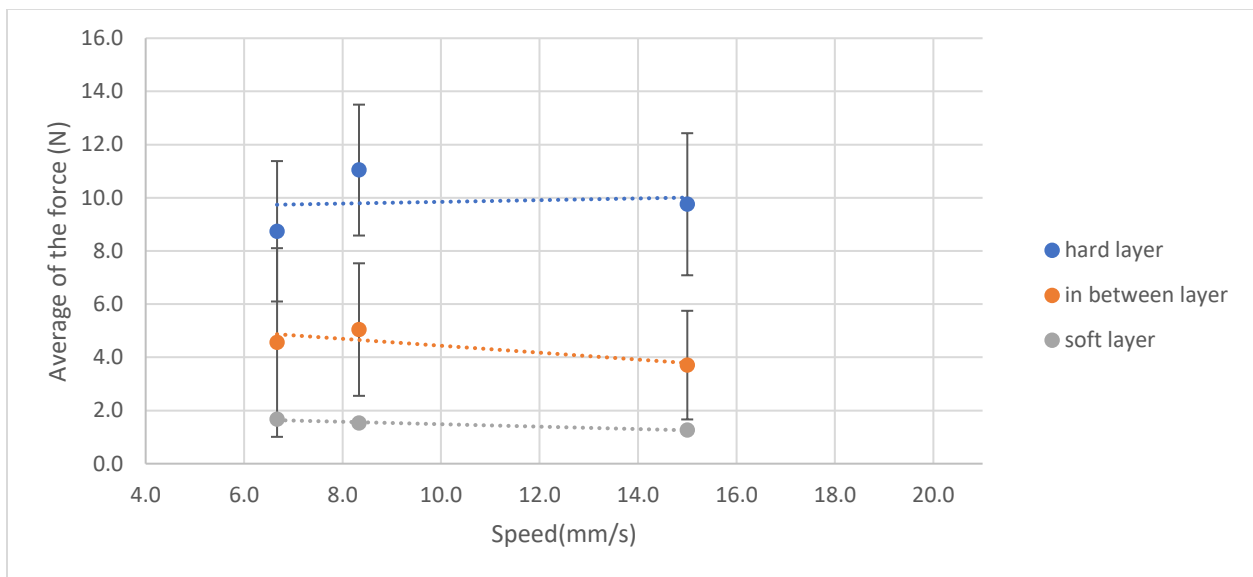

Figure 22. Average of the means of the plateau for each trial in three layers of the snow sample collected from site number 4 around the campus. The measurements were carried out at a speed between 6.7mm/s, 8.3mm/s, and 15mm/s.

The same procedure and investigation were followed in the last two figures. Multiple trials were carried out for several speeds (11.7mm/s, 13.3mm/s, and 16.7mm/s for figure 9. For figure 21 the speed values were 6.7mm/s, 8.3mm/s, and 15mm/s). Both data points follow the linear fit. Not surprisingly, the error bars are a bit longer at the hard layer data points compared to other layers. This could be due to the snow particles and how they were formed in the hard layer (the old layer basically). As it could be seen there is an increase of the force as we move from the soft layer towards the hard layer, and that it totally expected as the hard layer will have more resistance to the blade compared to the others.
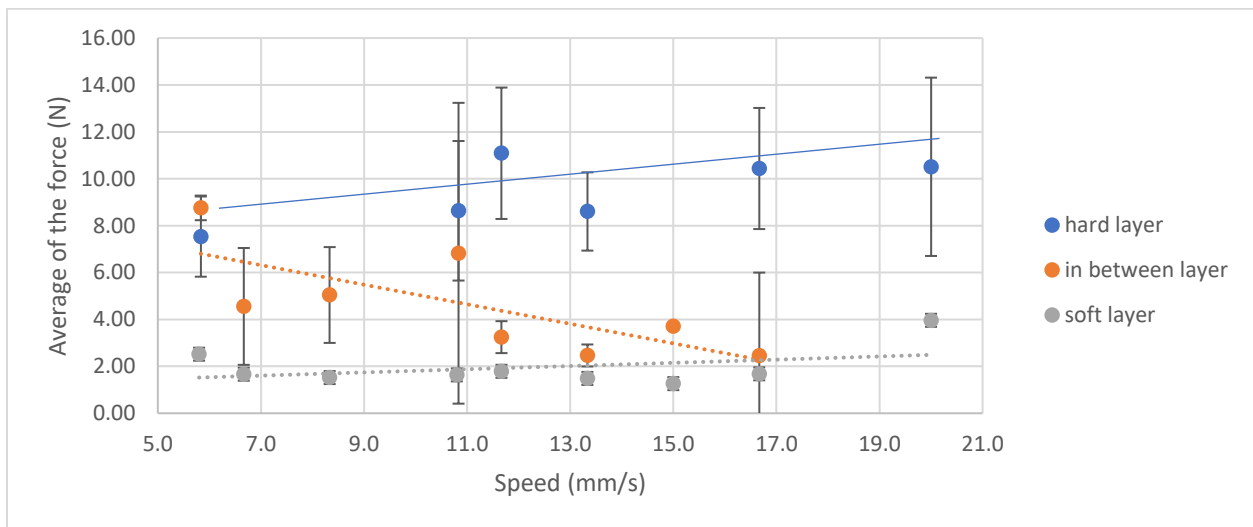

Figure 23. Average of the means of the plateau for each trial in three layers of the snow sample collected from sites around the campus. The measurements were carried out at a speed between 5.8mm/s and 20mm/s.

Figure 23 shows the average force versus insertion rate for the TRU snow samples (data were collected during January 27th, 31st, and February 3rd). The speeds range from about 5 to 20 mm/s and the data clearly show three distinct layers in the snow samples. Given the data was collected from slightly different areas and measurements made on different days, and then Figure 23 pieced together, the consistency of the data suggests the method of data collection did not introducing

significant changes to samples. While the best fit trendlines indicate some non-zero slope, overall, there is very little force dependence on the insertion speed. It also can be seen that the in between layer follow the linear fit more than the soft layer ($R^2 = 0.5 > 0.15$), and the hard layer comes last. Unsurprisingly the results display the force needed for the blade to go inside the hard layer was higher than the in between layer then the soft layer comes last. This was expected as the soft layer is easy to be destroyed by the blade insertion, also because the hard layer would definitely need more force to accommodate blade penetration into the layer.

It was concluded the BHG can differentiate between layers in snow samples collected from several sites around campus, where there were clearly visible. Now, we opted for collecting other samples from areas around Kamloops and compared them to the previous data.

Figure 24. Average of the means of the plateau for each trial in three layers plotted as function of the speed (mm/s). Snow samples were collected from Stake Lake area.

Snow samples were collected from a different area this time (Stake Lake with an elevation of 1335m, data were collected on March 3rd). Figure 24 displays data taken at three different speeds (6.7mm/s, 11.7mm/s, and 16.7mm/s). Layers in this sample were split into three

layers as they were visibly noticeable. Considering these data points some remarks can be made: most of the data points seems to be close to each other with no much of a difference. Also, the layers look similar, with a small variation between the bottom layer and the top layer. During the BHG measurements of this sample, some of the trials, especially the soft layer, experienced some fractures (the layer starts felling suddenly) occurred while inserting the blade repetitively, but they were not excluded from the data collection. This is maybe due to the fact data were collected after snowy days (on February 28, the total of snow was 0.9cm, with a total of 10.3 cm during the whole of February) (snowfall- monthly data of Kamloops, n.d.). While the difference between layers was visibly obvious, the BHG revealed a totally different result.
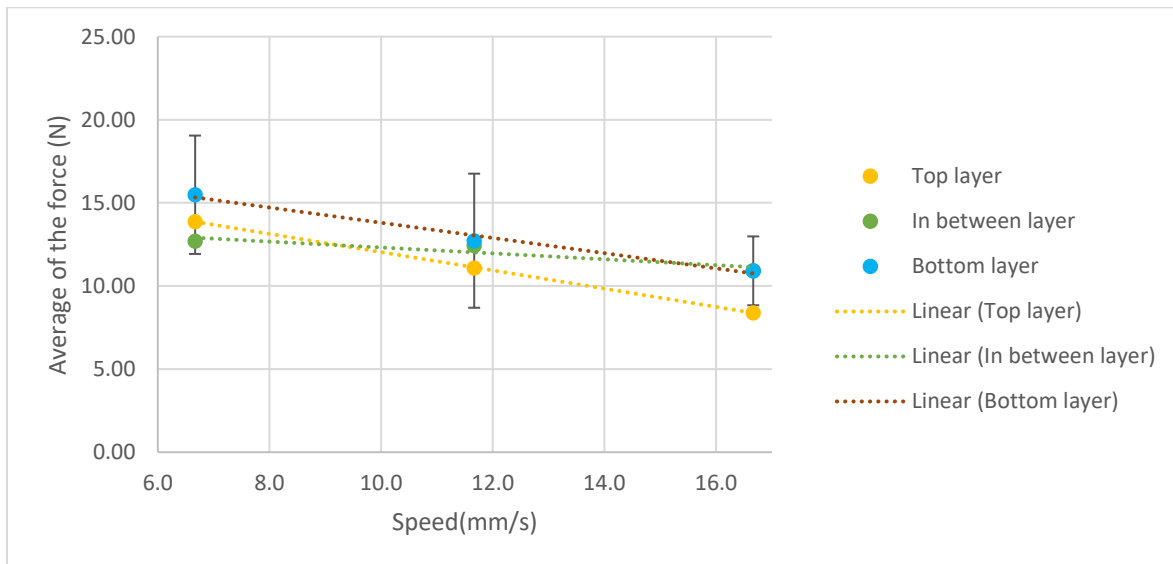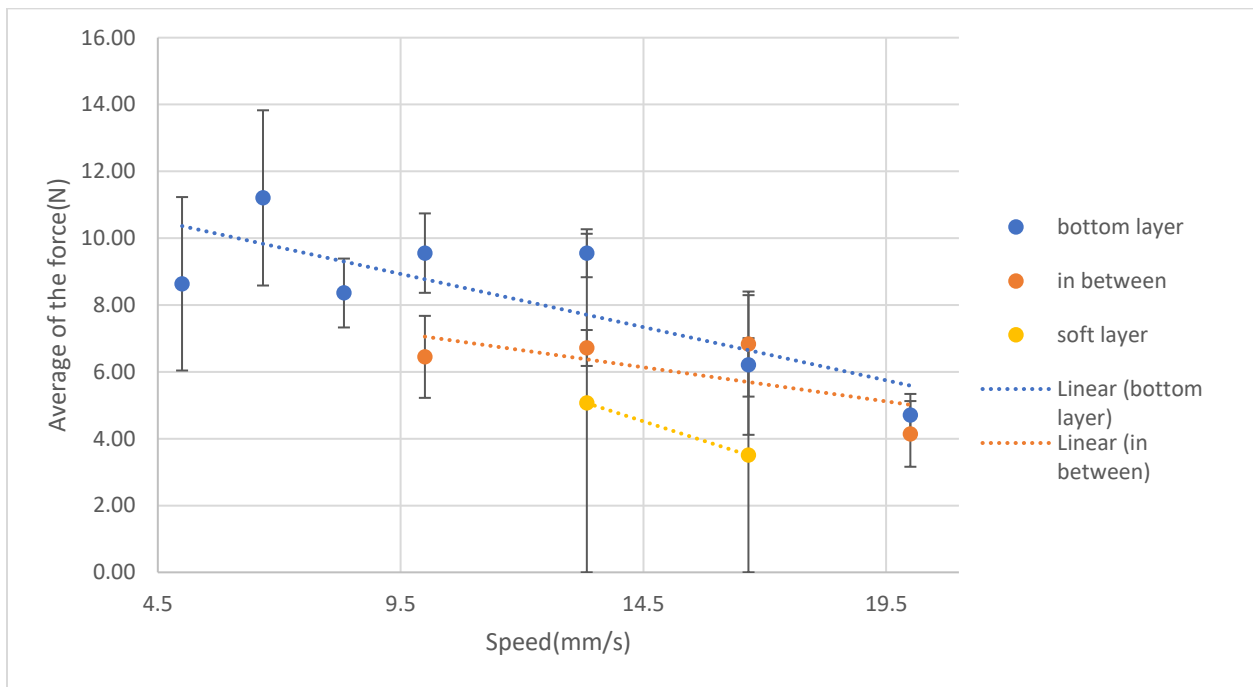

Figure 25. Average of the means of the plateau for each trial in three layers plotted as function of the speed (mm/s). Snow samples were collected from Sun Peaks area.

Figure 25 illustrates the results of the BHG measurements of samples collected from Sun Peaks area. The measurements were carried out at a speed value varying between 5mm/s and 20mm/s. In general, the harder the slab the higher the average of the plateau, and higher the

resistive force. However, in this snow sample there are more variations compared to other samples collected from around campus (Sun Peaks area has greater elevation. Mt. Tod summit elevation 2152m (Sun Peaks resort, n.d.)). Soft layer data points seemed to be less in number in comparison with the other data points, and that is due to the fragility of this layer, also it was not occupying a wide space. Another remarks, not all of the hard layer data point follows the linear fit. That is again maybe due to the snow sample history or the location where it was collected from, also the weather conditions (melting then freezing again). In the final analysis, even if we were able to see different layers visually, the blade's results showed that there is not much of difference between those layers.

Furthermore, in most of the hardness measurements graphs, it was noticed that there is a certain noise in the graphs after the blade insertion. Especially in the bottom layer at a low speed. In addition, a difference between TRU's snow samples results, Stake Lake, and Sun Peaks was revealed. That is due maybe to the snow sample history and the snow sample grains.

It is known that the bond characteristics of the different grain types determine the mechanical properties of the snow. (Colbeck, 1982). Colbeck also found that Metamorphism leads to a change in the mechanical properties of the snow as it is capable of modifying the shape of the snow crystals rigorously over time. Rounded grains and faceted crystals are the main endmember of snow metamorphism. When a snow layer is experiencing a temperature gradient of 10C/m or more, at this case the rounded grains will turn into facets. Brisk changes in weather conditions and thus changes in the temperature gradient induce the formation of transitional forms of rounded facets.

3.4 Summary

In this chapter we measured the density of the snow samples, then conduct measurements of the resistive force into several layers of the snow using the BHG. Ideally, we would conduct this chapter's measurements in the field, instead of collecting the snow data in the lab. Given that the fact of bringing the snow into the lab may initiate several errors (warming snow, warming blades), we tried to maintain the initial conditions to our best ability (keeping the blade out in the lab, and making sure the blade was untouchable with proper hands between trials). In spite of these circumstances, the data generated consistent results (provided that the snow samples were collected from around TRU on different days (January 27th, 31st, and February 3rd)).

The preliminary data of this chapter revealed that the force vs time graphs for snow exhibit different results than the other tested granular materials. In the snow graphs, the force has a sigmoidal increase followed by a plateau, then an unexpected increase again. In this thesis we focused only at the plateau occurring in the first 6 cm (length of the short copper blade is equal to 12cm).

After the investigation of the BHG into snow data collected from around the campus, we wanted to test other snow samples from different areas in Kamloops. Data collected from Stake Lake and Sun peaks point out less prominent layers in the graphs. This may be due to the history of the snow in those areas (Sun peaks data collected on Feb 10th, and Stake Lake data imported on March 3rd), also may be due to the elevation of the region. As we were more interested in the force results, this preliminary study gathered minimal weather data (days of snowfall, exterior temperature).

Due to the fact we needed to bring snow into the lab to complete the measurements, we were not able to replicate the testing as it would be done in the field. In the field a technician would insert the blade horizontally into the snow layers. The next chapter investigates blade hardness measurements when the blade is inserted horizontally.

Chapter 4: Horizontal Measurements

Most of the previous studies that were interested in investigating the snow hardness, they inserted their blade horizontally in the field. While all of our data collection and the BHG investigation were done vertically (vertical insertion of the BHG), in this chapter we want to examine the horizontal insertion of the BHG and compare the results to the vertical data. Using the same blade as the previous chapters, the horizontal measurements were carried out only for polystyrene and wet sand.

4.1 Materials & Methods

In order to investigate the resistive force in the polystyrene and wet sand horizontally, we flipped the texture analyzer onto its side, as shown in Figure 26. Same box used for the vertical measurements into the polystyrene was also used for the horizontal measurements in the wet sand. However, a different one was used for the polystyrene data collection. Both boxes were also flipped to the side with two different levels in the wet sand box, and three different levels in the polystyrene box. Some pieces of wood were added at the bottom of both boxes, for the levels to match the BHG while the insertion is occurring. Weights (2kg and 4kg) were added on top of the polystyrene box to increase compaction.

As the mechanical response of sand is largely dominated by the amount of water added to it, 10% and 15% moisture sand samples were created, following the same procedure mentioned in Chapter 3.

Figure 26. The box for the wet sand measurements marked with two levels in the cover, and the blade as it can be seen is matching level 2 before the insertion.

The Vernier force meter was again in this part to record the resistive force values in both polystyrene and wet sand. First the blade was inserted into the polystyrene box matching the first level with 2kg added to the top of the box for more compaction.

Polystyrene

4.2 Results

Figure 27 shows raw data of horizontal measurements of the polystyrene matching the third level marked on the box. The measurements were carried out with three different speeds (6.7mm/s, 13.3mm/s, and 20mm/s). The penetration force has an exponential trend and has been fitted to the relevant data (thick smooth line). Between trials, the polystyrene was mixed to maintain similar initial conditions. Five trials for each speed were accomplished and recorded on an excel spreadsheet, the average of c was calculated and plotted against the speed (mm/s).

The measurements were repeated at the same speed, in order to test the reproducibility. Figure 28 shows five trials for the short copper blade inserted into polystyrene horizontally at a

speed of 20 mm/s. The data shows a consistent behavior in all of the trials, but of course has variation due to the start time of the trials.
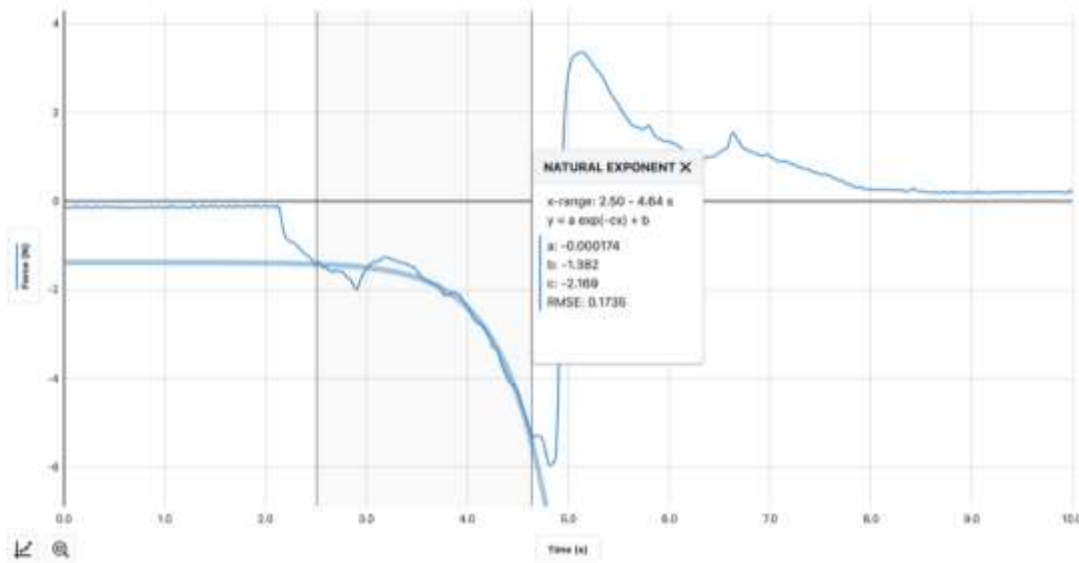

Figure 27. Data from the lab evaluations in polystyrene measured using Vernier force meter. The graph exhibits force versus time for a speed equal to 20mm/s, where the blade was inserted matching level 3 in the box, and with 2kg weight added on top. The light blue line indicates the fluctuations of the force in the polystyrene, and the solid blue line is an exponential fit to the data curve. The blade starts going inside the polystyrene at approximately 2.3s, and it goes back to the initial position at 5s.
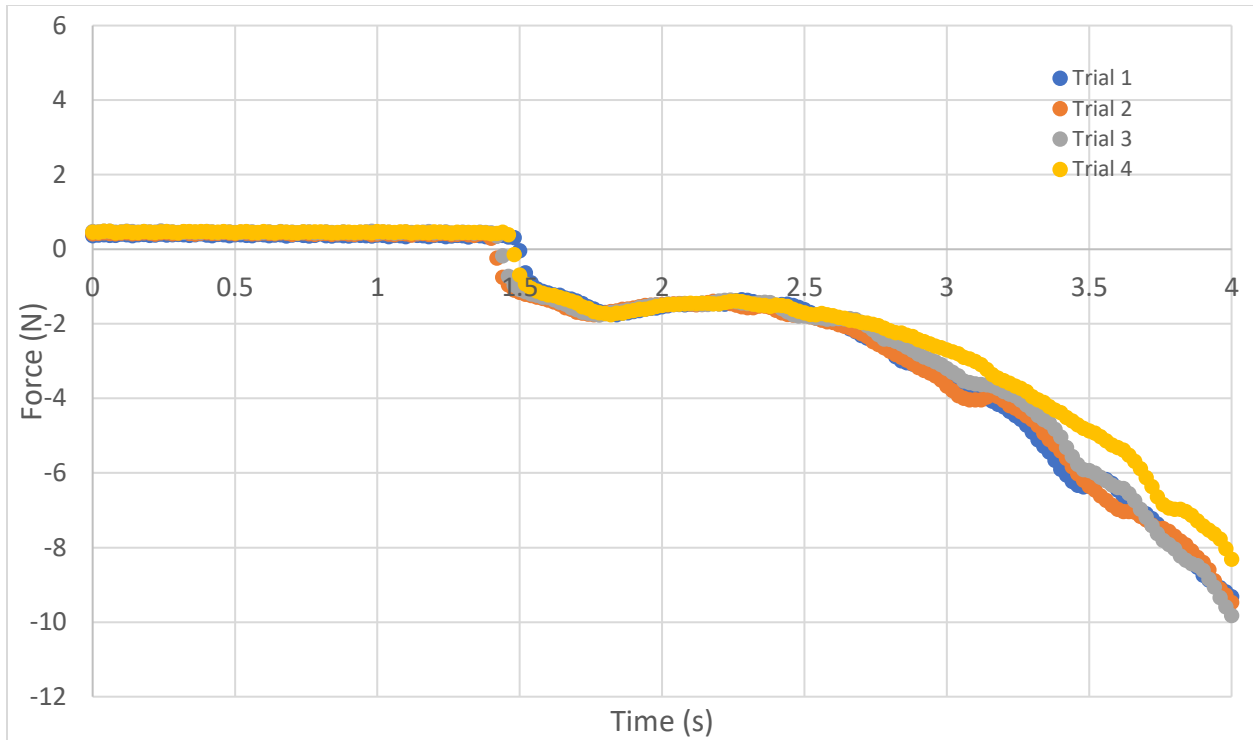
Figure 28. For five different runs, this figure exhibits the measured force as the blade is inserted at 20 mm/s into polystyrene horizontally. All trials display similar behavior.
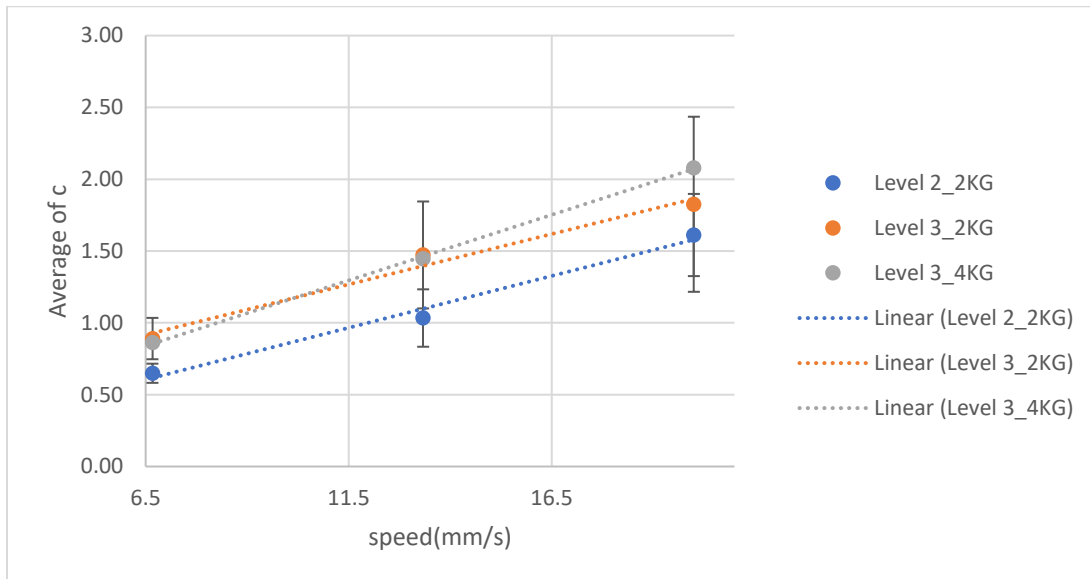

Figure 29. Horizontal measurements of the polystyrene. The blue series represents data of blade insertion at level 2 of the box with 2kg weight added on the top; orange series represents data taken at level 3 with a compaction of 2kg on top. Lastly, grey series shows data taken at level 3 with a weight of 4 kg on top of the box. The dashed line in the inset is the linear fit of this data.

Figure 29 exhibits the results of the horizontal polystyrene data while the blade was inserted into level 2 and 3 of the box and under a pressure of 2kg and 4kg. The figure also shows the average of c plotted as function of speed (mm/s). The data points are following the linear fit, with a little bit of variation. Mainly we can see a difference between level 2 and 3. However, when it comes to level 3 even if we have two different weights, the results are still the same, with a little bit of variation at the highest speed

Wet sand

The same procedure was followed in the wet sand data collection. The only difference is the box and the levels marked on the cover of it to compress the sand inside the box and preclude it from falling out (Fig.30). Five trials were carried out at three different speeds (6.7, 13.3, and 20 mm/s). Figure 30 shows how the wet sand looks like after applying some pressure on it to get a better sliding of the blade. In addition, the figure exhibits the appearance of wet sand after taking two measurements in both of the levels.

Figure 30. Wet sand moistens at 15% (with some pressure applied on it before measurements). The picture was taken after two horizontal measurements matching level 1 and 2.
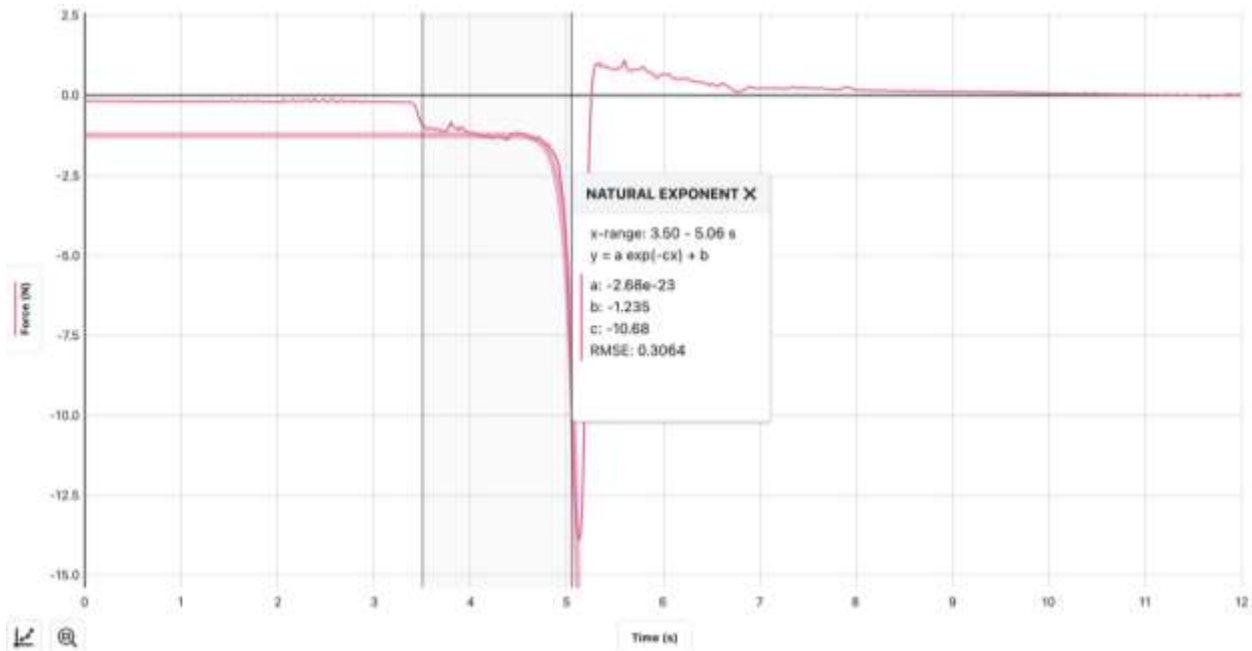
Figure 31. Raw data of wet sand containing 15% of moisture measured using Vernier force meter. The graph represents force versus time for a speed equal to 20mm/s, where the blade was inserted matching level 1 in the box horizontally. The time between 0 to 3.5s, the graph is matching the 0 N force line as the blade was not inserted yet (with some noises at the beginning of the insertion and at the end due to the blade was in contact with the cover of the box). After 3.5s the blade starts penetrating the sand until time equal to 5.1s when it stops and goes back to the initial position.

Figure 31 exhibits the force versus time data for the short copper blade at a speed of 20 mm/s. This graph shows a clear plateau, followed by exponential behavior of the force. The penetration force after 4s has an exponential trend and has been fitted to the relevant data (thick smooth line). When the blade rises from the bottom to the free surface, disturbances of the force profile are induced by the blade friction with the edge of the box, and this led to more fluctuations. Between trials, the wet sand was mixed, and a pressure was applied to it to make it easy for the blade insertion. For each trial, an exponential fit was added as the best fit of the data.
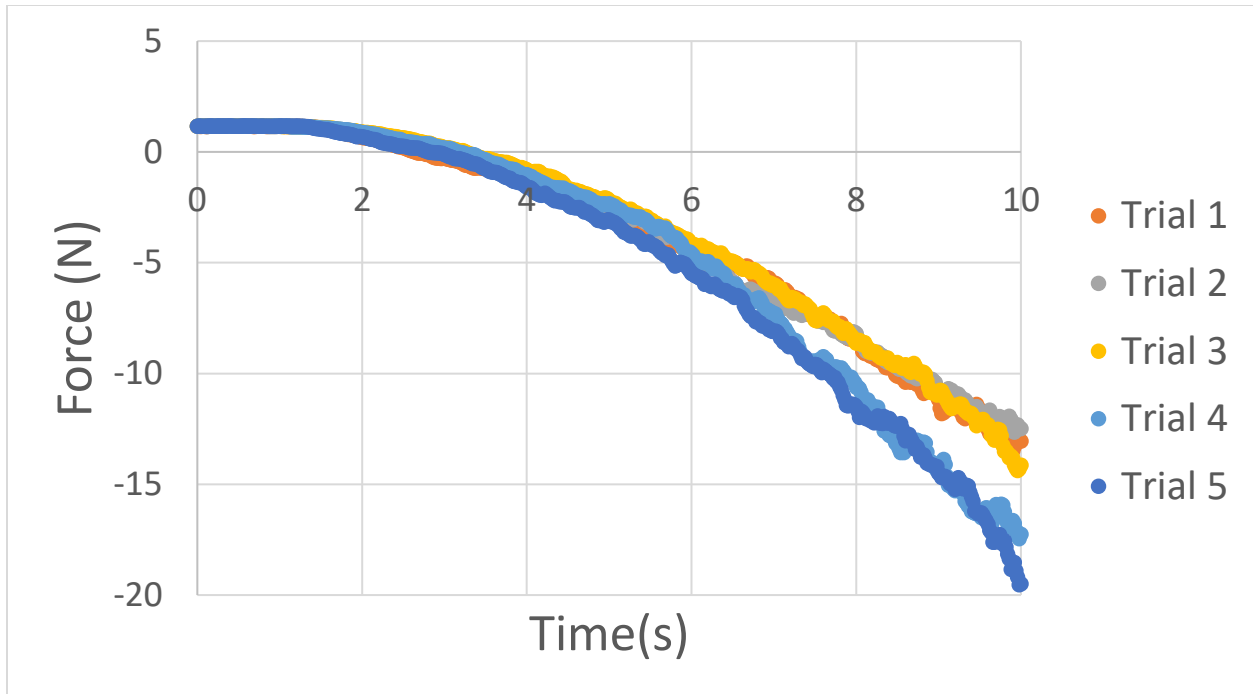
Figure 32. For five different runs, this figure shows the measured force as the blade is inserted at 20 mm/s into wet sand moisten at 15%. All trials display similar behavior.

For the purpose of testing the reproducibility of the measurements in wet sand horizontally, several trials were completed for each insertion speed. Figure 32 shows five trials for the short copper blade inserted into wet sand at a speed of 20 mm/s. The data shows a gradual increase in the force as the blade is inserted deeper into the sample box. Between trials, the wet sand was mixed and pressed to take the box shape. Not surprisingly, we see variation in the trials. That is due to difference in start time of trials.
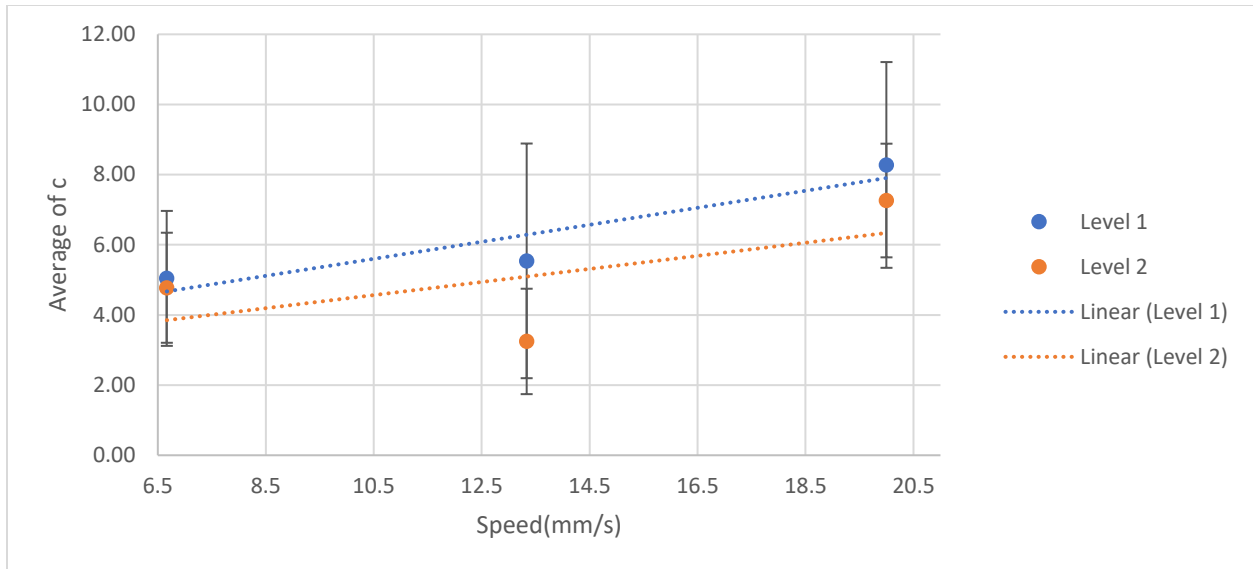
Figure 33. Horizontal measurements of the wet sand moisten at 15%. The blue series represents data of blade insertion at level 1 of the sand box; orange series represents data taken at level 2.

Figure 33 reveals the results of the wet sand data taken in level 1 then 2. Looking at these two data points we can make few remarks. The two levels show very little difference in force between them, and only slight dependence on the blade speed.

4.3 Summary

Considering the graphs of both polystyrene and wet sand some conclusions could be made: First, the polystyrene behavior while inserting the BHG horizontally shows similarity to the snow behavior. Especially if we take a look at the first graph of the polystyrene (Fig.27) at the time between 2.5s and 4.5s. Absolutely, the snow graphs have more noise in this area if we compare between both graphs, and it is totally expected as the snow has different layers and hardness as to the polystyrene. However, both of these granular materials have a low density. In other words, it is anticipated that they might show some similarities in behavior. In addition, what stands out is that the polystyrene's average of c versus the speed graphs maintain a linear trend in all of the levels and with two different weights added. Notably with 4kg, which means more pressure, the

trendline was perfectly linear. Similarly, average of c as function of the speed (mm/s) graphs were created for the wet sand data. Figure 35 summarize the results of the wet sand data at level one of the box. The trendline for these data is linear and more accurate than the second level. However, the error bars for the first level are relatively longer than the second level. This might be due to some factors: friction related to the percentage of the water, the capillary bridges between the grains, some remaining sand grains in the edge of the blade (even after cleaning up at the beginning of each trial), or friction of the blade with the cover of the box.

Chapter 5: Summary

The aim of this study was to investigate the reliability of the BHG in testing the properties of different granular materials: polystyrene, sand, and snow. This study provides preliminary results of BHG measurements of snow samples collected from areas around the Thompson rivers University campus and other areas around Kamloops city. At the same time, this research delves into examining the behavior of polystyrene, also investigating the impact of cohesiveness on granular material. In doing so, we investigated the behavior of dry sand then wet sand. The intent was to assess the efficiency of the blade hardness test in differentiating between cohesive and non-cohesive granular material (wet sand, dry sand). Similarly, to look at the capability of detecting the difference between the snow layers. At the end, test the horizontal measurements of the BHG and compare them to the vertical measurements.

Results from polystyrene experiments (vertical insertion of the thin blade) revealed that force depends linearly in distance. No matter which speed an individual can insert the blade into polystyrene, it will remain depending only on distance. By repeating the same procedure and by sustaining the same speed into several trials, the thin blade measurements demonstrate to maintain the reproducibility of the data. Additionally, the resistive force measurements into polystyrene were found to be sensitive to changes in blade composition.

Furthermore, dry sand data indicates that the resistive force depends exponentially into sand. Similar to the polystyrene findings, the BHG indicates the reproducibility of the measurements, and sensitivity while changing the blades and also the granular material. In the last part of chapter 2, vertical measurements of the BHG into wet sand were carried out. The results show an exponential increase of the force into the wet sand (moisten at different percentages). They also indicate that the BHG to be able to characterize the behavior of wet sand and detect the difference between cohesive and non-cohesive granular materials. The latter finding was proved

by the ability of the BHG in revealing changes into force profiles of wet sand with distinct percentage of moisture. In this chapter we also showed the force depended only on the depth of insertion, essentially meaning the speed of the blade may not be a factor in the field. This is in contrast to reported difference in BHG measurements in the field between slow insertion (20mm/s) and fast insertion (100mm/s) (Barsevskis 2022). It is interesting to note the work here only covers the slow insertion speed as reported by Barsevskis. Increasing the range of insertion speeds would be a recommended next step.

The preliminary results of polystyrene and sand raised the question of the ability of the BHG in examining the behavior of snow. In the last chapter, the output of the resistive force measurements into snow revealed that the BHG can differentiate between different snow layers, and the blade was found to require more force while penetrating the hard layer. This is valid for the data collected around Thompson Rivers University campus. However, other data from around Kamloops city (Stake Lake and Sun Peaks) showed a different conclusion; even if the snow samples had distinct layers that it could be visibly seen, the BHG reports no measurable differences in layers. On the other hand, the snow graphs show similar behavior in most of the layers. An exponential increase then stable at some point establishing a plateau followed by an unexpected increase again.

An investigation of the behavior of polystyrene and wet sand by horizontal insertion of the BHG was completed. The wet sand showed an identical behavior to the vertical measurements. At different levels of the sand box and with different percentages of moisture, the wet sand graphs indicate an exponential increase of the resistive force. On the other hand, the polystyrene exhibits a behavior similar to the snow. By taking a look at several polystyrene penetration force graphs, it was noted a resemblance at a certain interval of time with other snow graphs. After adding more

pressure to the polystyrene box, graphs of average of c in function of the speed displayed a linear behavior.

This thesis provides preliminary results and the method used by the BHG in examining the characteristics of the granular materials (polystyrene, dry and wet sand, snow). The BHG proved to be a promising tool for further investigations not only for investigation of different granular materials, but also in the forecasting of snowpacks. At the same time, this study contributes in helping researchers in the field to answer the question of does the speed of the insertion matters? In follow-up studies a use of another tool (lighter than the texture analyzer) to control the speed of insertion would be appropriate to find a possible parametrization of the features of the texture analyzer (maybe in a smaller version). Furthermore, to optimize the presented results it is crucial to find locations with old layers or of a certain height, with keeping in mind to gather more weather data and maintain the same temperature of the blade through the data collection. Also, a comparison between vertical and horizontal insertion of the blade in the field could be another suggestion, especially for snow. Consequently, all of the previous suggestions would improve the quality of the BHG results and use, precisely that the BHG is small and lightweight, and an inexpensive tool that can be utilized in the laboratory or in the field with objective results and consistent.

Bibliography

Barsevskis, P. (Oct 2022). *M. Sc. Thesis (unpublished).* Kamloops: Thompson Rivers University.

Borstad, C. &. (2010). A paint scraper hardness blade. *International Snow Science Workshop*.

C.P. Borstad, D. M. (2011). Thin-blade penetration resistance and snow strength. *Journal of Glaciology*.

Carlson, J. (2008). *complex systems*. Retrieved from web physics usbc: http://web.physics.ucsb.edu/~complex/research/granular.html

Floyer, J. &. (2006). Empirical analysis of snow deformation below penetrometer tips. *In Proceedings of the International Snow Science Workshop*, 1-6.

Floyer, J. &. (2006). Empirical analysis of snow deformation below penetrometer tips. *n Proceedings of the International Snow Science Workshop*, 1-6.

Floyer, J. A. (2008). Avalanche weak layer tracing and detection in snow penetrometer profiles. *In Proceedings of the 4th Canadian Conference on Geohazards, Quebec City, QC*, 161-168.

Goncü, F. (2012). Mechanics of Granular Materials: Constitutive Behavior and Pattern Transformation. *Delft Center for Computational Science and Engineering (DCSE)*.

Goodfellow. (2008). Retrieved from http://www.goodfellow.com/E/Polystyrene-Granule.html

H.C.S. (1970). Quantitative Evaluation of Climatic Factors I.ll Relation to Soil Moisture Regime. *Highway research record* .

Herminghaus, S. S. (2012). Wet granular matter: a truly complex fluid. *Soft matter*.

Jür̈g Schweizer, T. W. (2001). Snow profile interpretation for stability evaluation. *Cold Regions Science and Technology*, 179-188.

Klein, G. (1950). Canadian survey of physical characteristics of snow-covers. *National Research Council of Canada. Division of Building Research*.

M.Haynes, W. (2020, August). Retrieved from https://www.aqua-calc.com/page/density-table/substance/polystyrene-blank-foam

McClung, C. B. (2010). A PAINT SCRAPER HARDNESS BLADE. *International Snow Science Workshop*.

Mcclung, C. B. (2011). Thin-blade penetration resistance and snow strength. *Journal of Glaciology*.

McClung, F. P. (2016). USING A THIN-BLADE TOOL FOR MEASURING SNOW HARDNESS AND CHANGE IN STRENGTH OF BURIED SURFACE HOAR. *Proceedings, International Snow Science Workshop, Breckenridge, Colorado*.

N. J. Kinar, J. W. (2015). Measurement of the physical properties of the snowpack. *AGU publications*.

Quervain, d. M. (1950). Die Festigkeitseigenschaften der Schneedecke und ihre Messung. *Geofisica Pura e Applicata*, 179–191.

Shinichiro Miyai1, 2. ·. (2019). Influence of particle size on vertical plate penetration into dense cohesionless granular materials (large-scale DEM simulation using real particle size). *Granular matter*.

snowfall- monthly data of Kamloops. (n.d.). Retrieved from https://kamloops.weatherstats.ca/charts/snow-monthly.html

Stull, R. (2018). *Weather for Sailing, Flying & Snow Sports* . Retrieved from Density of Newly-Fallen Snow : https://www.eoas.ubc.ca/courses/atsc113/snow/met_concepts/07-met_concepts/07b-newly-fallen-snow-density/

Sun Peaks resort. (n.d.). Retrieved from https://www.sunpeaksresort.com/ski-ride/the-mountain/trail-maps-stats

Thom, H. (1970). Quantitative Evaluation of Climatic Factors I.ll Relation to Soil Moisture Regime. *Highway research record*.

Umbanhowar, H. M. (2000). Does the granular matter? *Proceedings of the National Academy of Sciences*, 24.

Way, R. J. (2021). A low-cost method for monitoring snow characteristics at remote field sites. *the cryosphere*.